IEEE Access
Multidisciplinary | Rapid Review | Open Access Journal

Received October 13, 2020, accepted October 28, 2020, date of publication November 10, 2020,
date of current version December 10, 2020.

Digital Object Identifier 10.1109/ACCESS.2020.3037048

Individualistic Dynamic Handover Parameter Self-Optimization Algorithm for 5G Networks Based on Automatic Weight Function

IBRAHEEM SHAYEA[1], MUSTAFA ERGEN[1], AZIZUL AZIZAN[2], MAHAMOD ISMAIL[3], (Senior Member, IEEE), AND YOUSEF IBRAHIM DARADKEH[4]

[1]Electronics and Communication Engineering Department, Faculty of Electrical and Electronics Engineering, Istanbul Technical University (ITU), 34467 Istanbul, Turkey
[2]Advance Informatics Department, Razak Faculty of Technology and Informatics, Universiti Teknologi Malaysia, Kuala Lumpur 54100, Malaysia
[3]Department of Electronics, Electrical and System Engineering, Universiti Kebangsaan Malaysia, Bangi 43600, Malaysia
[4]Department of Computer Engineering and Networks, College of Engineering at Wadi Addawasir, Prince Sattam Bin Abdulaziz University, Al Kharj 11991, Saudi Arabia

Corresponding author: Ibraheem Shayea (ibr.shayea@gmail.com; shayea@itu.edu.tr)

This research has been produced benefiting from the 2232 International Fellowship for Outstanding Researchers Program of TÜBİTAK (Project No: 118C276) conducted at Istanbul Technical University (ITU), and it was also supported in part by Universiti Teknologi Malaysia (UTM), Research University Grant Scheme Tier 2, PY/2019/00325.

ABSTRACT Ensuring a reliable and stable communication throughout the mobility of User Equipment (UE) is one of the key challenges facing the practical implementation of the Fifth Generation (5G) networks and beyond. One of the main issues is the use of suboptimal Handover Control Parameters (HCPs) settings, which are configured manually or generated automatically by certain self-optimization functions. This issue becomes more critical with the massive deployment of small base stations and connected mobile users. This will essentially require an individual handover self-optimization technique for each user individually instead of a unified and centrally configured setting for all users in the cell. In this paper, an Individualistic Dynamic Handover Parameter Optimization algorithm based on an Automatic Weight Function (IDHPO-AWF) is proposed for 5G networks. This algorithm dynamically estimates the HCPs settings for each individual UE based on UE's experiences. The algorithm mainly depends on three bounded functions and their Automatic Weights levels. First, the bounded functions are evaluated, independently, as a function of the UE's Signal-to-Interference-plus-Noise-Ratio (SINR), cells' load and UE's speed. Next, the outputs of the three bounded functions are used as inputs in a new proposed Automatic Weight Function (AWF) to estimate the weight of each output bounded function. After that, the final output is used as an indicator for optimizing HCPs settings automatically for a specific user. The algorithm is validated throughout various mobility conditions in the 5G network. The performance of the analytical HCPs estimation method is investigated and compared with other handover algorithms from the literature. The evaluation comparisons are performed in terms of Reference Signal Received Power (RSRP), Handover Probability (HOP), Handover Ping-Pong Probability (HPPP), and Radio Link Failure (RLF). The simulation results show that the proposed algorithm provides noticeable enhancements for various mobile speed scenarios as compared to the existing Handover Parameter Self-Optimization (HPSO) algorithms.

INDEX TERMS Handover parameter optimization, mobility robustness optimization, self-optimization algorithm, handover control parameters, Hysteresis, handover margin, Time-to-Trigger (TTT), LTE-Advanced Pro, 5G networks.

I. INTRODUCTION

The Handover Parameter Self-Optimization (HPSO) is one of the significant Self-Optimization Network's (SON) functions that have been introduced by the 3rd Generation Partnership Project (3GPP) in Fourth Generation (4G) and Fifth Generation (5G) mobile technologies [1]–[8]. In the 4G system, HPSO is also known as Mobility Robustness Optimization (MRO) function, and it is heading to be more advanced in 5G mobile systems [2]–[8]. This function aims to adjust the

The associate editor coordinating the review of this manuscript and approving it for publication was Shaoyong Zheng.

Handover Control Parameters (HCPs) settings automatically in order to solve handover problems [9]. Handover mainly occurs when the User Equipment (UE) moves in between two cells during connected mode. This is intended to preserve the connection received by the UE [10]. The suboptimal settings of HCPs may consequently contribute to high rates of Handover Probability (HOP), Handover Ping-Pong Probability (HPPP) or Radio Link Failure (RLF), which will collectively produce increased redundancy leading to wastage of network resources. Therefore, it is important to highlight the central objective of the HPSO algorithm, i.e. to reduce the HOP, HPPP, and RLF that may be impacted from HCP settings tuning. Therefore, issues associated with high HOP, HPPP, and RLF settings should also be addressed and reduced significantly by implementing efficient HPSO algorithms.

Consequently, several algorithms have been proposed in the literature to optimize HCP settings [11]–[32]. Different methodologies were used with these algorithms and investigated in various environments. In [11], machine learning and data mining techniques were proposed for optimizing handover parameters. They were evaluated over the Long-Term Evolution (LTE) system in a building environment. In [12], a high mobility SON function was introduced to shorten the multi-layer time in the LTE system. It performs optimization by estimating user mobility behaviors based on data measurements that were previously collected by users. In [13], an algorithm was introduced to adaptively adjust the Handover Margin (HOM) according to the position of the user in the cell. As the user gets closer to the cell edge, the HOM further decreases. In [14], Enhanced Mobility State Estimation (EMSE) was introduced to optimize HCPs (i.e. Time-To-Trigger (TTT) and HOM) based on handover types and speed of users.

Moreover, the Fuzzy Logic Controller (FLC) was proposed to adaptively modify the HOM level while a fixed value is set for TTT [15]. The HOM level is adjusted by the FLC based on two control input metrics: the Drop Call Probability (DCP) and the Handover Ratio (HOR). Another gradient method and cost function-based MRO scheme was also proposed for LTE femtocell [16]. It performs optimization based on a cost function consist of various metrics. The cost function is calculated as a function of HPPP numbers, continuous handover, too early handover, too late handover, and handover to the wrong cell. In [17], the HCP settings are tuned according to the average Handover Performance Indicator (HPI) by Weighted Performance based on the Handover Parameter Optimization (WPHPO) algorithm. The WPHPO algorithm is evaluated as a function of Handover Failure Probability (HFP), HPPP, and DCP. The studies in [18] and [24] proposed SON algorithms, but only one HCP was considered in their analysis. Whereas in [17] and [19], techniques in modifying both the HOM and TTT were proposed, however, the impact on the UE speed were not investigated. In [20] and [23], the inter-system handover parameter optimization was considered in the investigation. Finally, in [21] and [22], investigations on some performances of intra-frequency LTE handovers are explained. However, no efficient handover SON algorithms were in the papers mentioned can estimating the optimal HCP settings.

Even though these algorithms contribute to enhance handover performance, they are not robust nor ideal in selecting appropriate HCP values in the 5G system. The existing algorithms are inefficient due to various reasons. One of the main reasons is that most of these algorithms were developed for the 4G technology, which has different specifications and requirements in comparison to the 5G technology. As a result, the existing algorithms developed for previous cellular networks may not be efficient to be implemented in 5G networks. Thus, further investigations are required for 5G networks with various mobility and deployment scenarios. Eventually, efficient and validated algorithm(s) can be recommended for further development or use in 5G networks. In addition, all the earlier mentioned algorithms were designed to operate based on a central optimization model. This means the optimization operation is accomplished based on the performance of the entire network, and not on the bases of individual user experience. The algorithm adjusts HCP settings at the Base Station (BS) for the entire system and then the handover for all mobile users is controlled by utilizing the same HCP settings. This central optimization may lead to increased handover issues for some users. This is because not all mobile users require the optimization process at the same time and in the same direction. Some users may require optimization at the current time, while other users may need optimization at a different time. Also, at time T, some users may require optimization in the upper direction, while other users may need it at a different direction. As a result, a central optimization operation is a critical issue that must be addressed in 5G networks. The issue becomes even more critical due to the small coverage offered by 5G BS and the required support for high mobility speeds (500 km/r). Moreover, the need for ultra-reliable communication in 5G networks is necessary for some remote-control users. Thus, central optimization will not be the best solution for 5G networks. Another issue is the type of HCPs considered for optimization. Some existing algorithms do not optimize all HCPs. For example, some algorithms only optimize one HCP (the HOM), such as in [15], [18], [24]. This may cause an increased in handover as well. Utilizing a fixed TTT may also lead to another handover issue which HPSO aims to address. Therefore, more efficient HPSO algorithms should be developed and validated for 5G networks.

In this paper, a new algorithm is developed to adaptively estimate the HCP settings for each UE independently. The proposed algorithm estimates HCP settings based on the Weight Function, which depends on three bounded functions and the weight of each bounded function. The bounded functions are evaluated as functions of Signal-to-Interference-plus-Noise-Ratio (SINR), load, and UE speed. The weight of each bounded function is calculated based on a proposed dynamic mathematical function that depends on the output of the three bounded functions. The proposed algorithm was then investigated based on a simulation study using

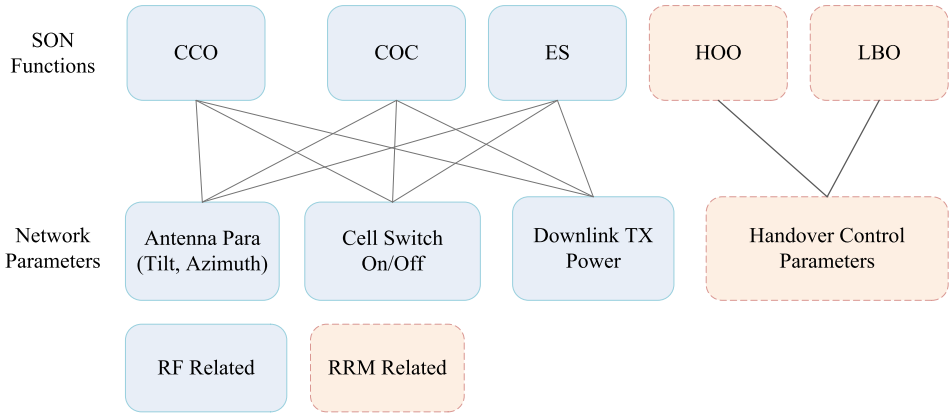

FIGURE 1. Self-Optimization functions and their relationship with network control parameters [33].

the MATLAB 2020a software. It is further compared with three different algorithms from the literature. The results indicate that the developed algorithm provides noticeable enhancements compared to other algorithms, as illustrated in the results section.

The rest of this paper is organized as follow: Section II describes the proposed handover parameter self-optimization algorithm. Section III presents the system model and the simulation scenario. Section IV discusses the key performance indicators briefly. Section V discusses the simulation results. Finally, Section VI concludes the paper.

II. RESEARCH OVERVIEW AND MOTIVATION

The SON has been standardized and applied as a fundamental feature in Fourth Generation (4G) and Fifth Generation (5G) mobile technologies [6], [34]–[37]. This feature was introduced by the 3GPP initially in LTE (Release 9 (Rel.9)). Then, it had been developed further in LTE-Advanced (Rel.10 to Rel.14) with the existing of Carrier Aggregation (CA) technique [38]–[41]. In 5G systems, (3GPP Rel.14 to Rel.17) [2]–[4], [42]–[46], the SON has become more advanced and further developments are continuously ongoing. Rel.14 is considered to be the first 5G standardization [47], while Rel.15 was introduced as the first full set of 5G standards for International Mobile Telecommunications 2020 (IMT-2020) standard [48]. The main focus of SON is to maintain the network quality and system execution with minimal manual intermediation from the administrator [45]. SON is mainly introduced to reduce the Operating Expenditure (OPEX) of the network controlling functions. This feature has become an automated technique that is necessary to be implemented in future networks. This is due to the massive growth of mobile connections and small BSs that will be deployed in future which will lead to building ultra-dense cellular networks. Such networks require more efficient, automatic and robust management functions. Otherwise, the network operation cost will be high, and the network performance will not be at the desired level where future networks targets to deliver. Thus, implementing advanced SNO functions are required to efficiently enhance network performance, decrease the administrative needs by network operators, as well as managing the complexity of network maintenance and operation. The main function implemented by the SON is to automatically adjusts network parameters based on the measurements and performance of UE and evolved NodeB (eNB).

In SON, several functions have been introduced to optimize network parameters, as illustrated in Figure 1. Each function performs specific optimizations to achieve different objectives. However, two SON functions focus on optimizing HCPs settings for different purposes. One function is known as the HPSO function, while the other is known as the Load Balancing Self-Optimization (LBO) function [5], [49]. The HPSO function optimizes HCPs to address mobility issues, while the LBO function optimizes HCPs to cater traffic issues. Within this study we will only focus on the HPSO function.

The HPSO function has been introduced by 3GPP as HOO where it is also sometimes termed as MRO [1]–[8]. The HPSO adjusts the HCPs automatically to address the issues arising from users' mobility [9]. The suboptimal settings of HCPs may consequently contribute to high HOP, HPPP or RLF, which will collectively produce increased redundancy due to the wastage of network resources. Therefore, it is important to highlight the central objective of the HPSO algorithm: to reduce the number of HOP, HPPP, and RLF that may arise by tuning HCP settings. The high HOP, HPPP, and RLF should be addressed by implementing efficient HPSO algorithms. There are several techniques that have been proposed to perform the automatic optimization for the HCP settings in the literature [11]–[32]. Each technique proposed different method where investigation was performed in different environments with different system settings and network scenarios. Although these solutions have contributed in reducing the mobility issues further, but to the best of our knowledge there is no optimal solution available yet. This due to several factors as explained in our previous survey paper [1]. Moreover, there is a main issue that has not been addressed yet due to the

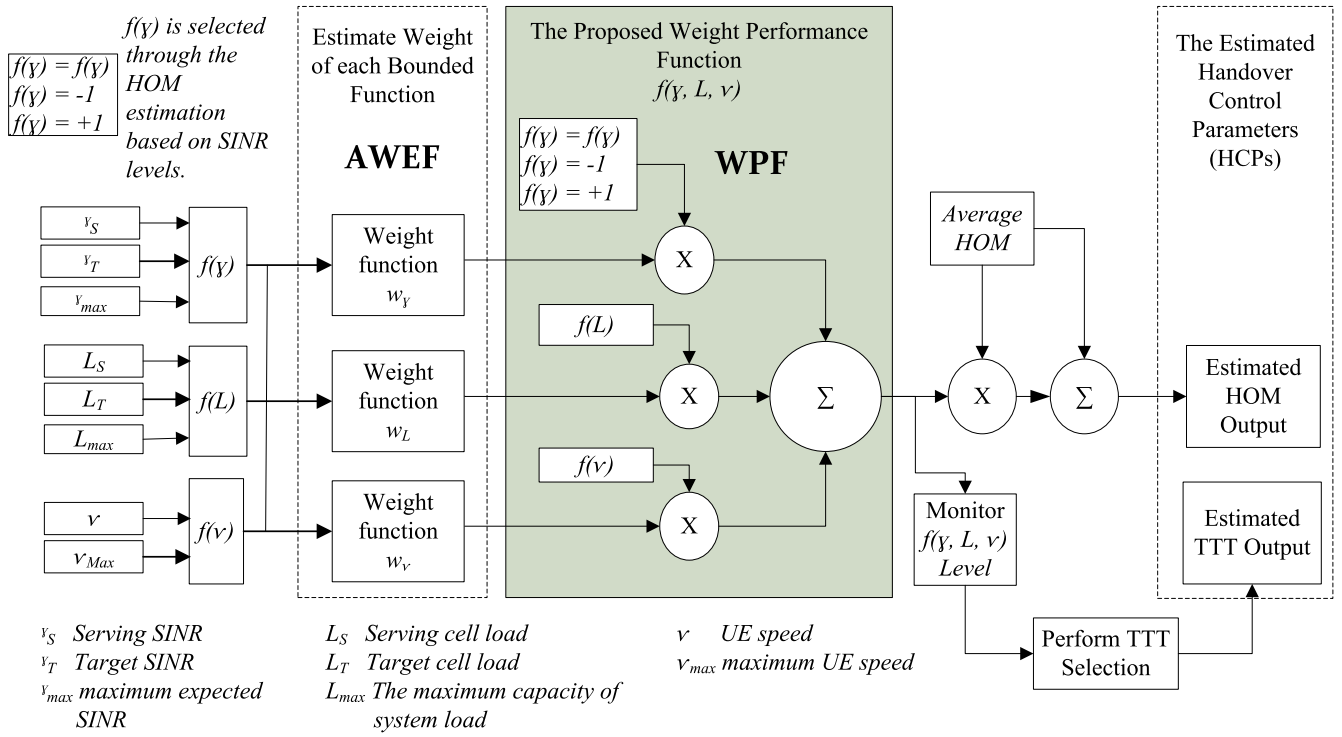

FIGURE 2. Proposed IDHPO-AWF algorithm for dynamically estimating HCPs settings for each UE independently.

deficiencies of centralized optimization operation [1]. Also, the existing solutions were developed for 4G technology, which may not be efficient for 5G networks as it has different specifications and requirements compared to the previous 4G technology [1]. Moreover, the partial self-optimization operation and another outstanding issues need to be addressed [1] to enable efficient solutions for 5G networks.

III. PROPOSED SOLUATION

The proposed function aims to automatically adjusting HCPs settings automatically and dynamically for each UE individually. This will contribute significantly for estimating more appropriate HCPs for each UE based on its experiences independently. Also, it will contribute significantly for avoiding the negative impact on the other UEs those are not requiring any change to their HCPs settings. This will enhance the RSRP, reduce the HPPP and RLF. That in turn lead to a significant enhancement in offering more stable communication during UEs' mobility.

This section describes the proposed Individualistic Dynamic Handover Parameter Optimization algorithm based on an Automatic Weight Function (IDHPO-AWF), as illustrated in Figure 2. The proposed algorithm explained in details in two main subsections. The first subsection explains the proposed Weight Function with the bounded functions and the automatic estimator weight model. The second subsection illustrates the dynamic estimation for HCPs (HOM and TTT) based on the Weight Function illustrated in the first subsection.

A. PROPOSED WEIGHT FUNCTION

An IDHPO-AWF algorithm is proposed to dynamically estimate suitable HCP values for each independent UE. It considers several influencing factors (metrics) such as SINR, cell load, and UE speed. These three factors are selected due to their direct impact on making handover decision. The handover decision is usually made based on the received signal level (Reference Signal Received Power (RSRP) or SINR) and the load conditions of both the serving and target BSs. The mobile velocity change has a direct impact on the SINR levels. As a consequence, the HCPs must be adjusted accordingly. Thus, the proposed IDHPO-AWF algorithm adjusts HCP settings based on the variations of these three metrics. Since the selected metrics have different variations and impacts, formulating them in one Weight Function will provide more accurate and diverse results based on the variation and weight of each considered factor. However, formulating different metrics in one Weight Function must be represented in a form that provides bounded results for all input metrics. Therefore, the three main input metrics in the proposed Weight Function formula must be formulated in a type of boundary function, f_b. The boundary function means that the output of each bounded function must be between a defined range; for example, $f_b \in [-1, 1]$. This is because they will be used in one weight formula. Therefore, the Weight

Function will be calculated as a function of three bounded sub-functions. Since each bounded function may provide a different impact, the weight of each bounded function must be considered. Therefore, Weight Function is calculated as a function of three bounded sub-functions and their weights. These three bounded sub-functions can be represented by SINR $f(\gamma)$, Load $f(L)$, and UE's speed $f(v)$. Their weights are represented by ω_γ, ω_L and ω_v, respectively. Thus, the proposed Weight Function is mathematically expressed by Eq.1:

$$f_{WF}(\gamma, L, v) = \omega_\gamma f(\gamma) + \omega_L f(L) + \omega_v f(v) \quad (1)$$

For simplicity, Eq.1 can be divided into two parts. The first part is the boundary sub-functions $\{f(\gamma), f(L), \& f(v)\}$, while the second part is the weight of each sub-function $\{\omega_\gamma, \omega_L, \omega_v\}$. These two parts (i and ii) are illustrated in the following subsections:

1) THE BOUNDED FUNCTIONS

This section explains the formulation of the three bounded functions.

a: BOUNDED SINR FUNCTION

Switching the connection from one BS to another is performed by making a handover decision at the serving BS. This is accomplished by using a handover decision algorithm. Several handover decision algorithms are presented in the literature. They were designed according to different metrics and diverse conditions. The most usable algorithm is based on the received signal strength. This algorithm makes the decision based on the differences between the received signal strength of the serving and selected target BSs and the specific handover margin. The signal strengths are measured at the user's side and then reported to the BS, which then decides to initiate the handover preparation. This occurs when the target received signal strength becomes greater than the serving received signal strength by the handover margin level in a specific period of time (TTT).

The best parameter to represent the received signal strength is the SINR since it includes the noise and the interferences in its calculations. For that reason, the SINR is considered as an input metric in the proposed Weight Function. Thus, the boundary SINR function can be expressed as the differences between the serving and target SINR levels. Since the SINR is used in Weight Function, its output must be bounded between $[-1, 1]$. To achieve this target, the differences of SINR should be divided by the maximum SINR expected level. That will make the output of $f(\gamma)$ to be between two bounded values: $f(\gamma) \in [-1, 1]$. Thus, the bounded SINR function $f(\gamma)$ in Eq.1 can be calculated as a function of the target and serving SINR (γ) ratios, as expressed in Eq.2:

$$f(\gamma) = \left(\frac{\gamma_T}{\gamma_{Max}}\right) - \left(\frac{\gamma_S}{\gamma_{Max}}\right) \in [-1, 1] \quad (2)$$

where, γ_S and γ_T represent the SINR over the serving and target carriers, respectively, while γ_{Max} represents the maximum SINR expected to be received at the UE side. Since the acceptable SINR level ranges between -10 to 30 dB, the maximum SINR value is assumed to be 30 dB ($\gamma_{Max} = 30$) in this study.

b: BOUNDED LOAD FUNCTION

The load function is another significant metric that must be considered. The justification of considering the load as an input metric in the Weight Function (Eq.1) is due to two main reasons. First, after the handover decision is made and the handover request is sent to the target BS, it will decide to either accept or deny the handover request based on the -availability of its resources. Second, balancing load between cells is one cause for making the handover. That means some of the users at the cell boundaries are allowed to switch their connections to neighboring cells in order to balance the load between cells. Therefore, the cell load becomes a significant metric in the proposed Weight Function. It will be used in the form of a boundary function.

The load boundary function can be evaluated as a function of serving and target cell loads. Since the equalization of the minimum and maximum borders of all boundary functions is required in Eq.1, we must divide the load differences by the maximum cell load capacity. This is needed to limit the output of $f(L)$ between two bounded levels: $f(L) \in [-1, 1]$. Thus, the bounded load function, $f(L)$, can be represented as the difference between the target and serving load ratio. The target load ratio is defined as a ratio of the target cell's load to the maximum cell's Load capacity (L_{max}). Similarly, the serving load ratio is defined as a ratio of the serving cell's load to the maximum cell's Load capacity (L_{max}). Thus, the cell boundary function, $f(L)$, in Eq.1 can be represented by Eq.3:

$$f(L) = \left(\frac{L_T}{L_{max}}\right) - \left(\frac{L_S}{L_{max}}\right) \in [-1, 1] \quad (3)$$

where L_T and L_S represent the target and serving cell loads, respectively.

c: BOUNDED SPEED FUNCTION

Mobile speed is a significant metric that influences the handover performance. This is because high mobile speed linearly increases the handover probability. As a result, the mobile speed is considered as an input metric in the proposed Weight Function. The bounded speed function expressed by $f(v)$ in Eq.1 can be evaluated as a function of the UE's movement speed, v. Since the output of $f(\gamma)$ *and* $f(L) \in [-1, 1]$, is bounded, the output of $f(v)$ must be similarly bounded $f(v) \in [-1, 1]$. To formulate this target in a mathematical formula, the logarithm function was used. Thus, after empirical investigations of the logarithm function, the bounded speed function, $f(v)$, in Eq.1 is represented by Eq.4:

$$f(v) = 2 \cdot log_2\left(1 + \frac{v}{v_{max}}\right) - 1 \in [-1, 1] \quad (4)$$

where v_{max} represents the maximum expected speed of UE, which is assumed to be constant ($v_{max} = 140$ km/hour) in

this study. In scenarios where the maximum mobile speed is expected to exceed this limit (140km/hr), the constant speed value can then be changed accordingly.

2) THE PROPOSED AUTOMATIC ESTIMATOR WEIGHT MODEL

This sub-subsection illustrates the second part of Eq.1, which is the weight of each boundary function. In the literature [17], [50], the Weight Function was used in different forms with various applications. To the best of our knowledge, all functions employed static weight values. A fixed value was manually defined for each weight. Previous studies had assigned different constant weight values. Unfortunately, there is no formulated mathematical expression to automatically estimate the weight of each factor (metric) considered in any weight or cost function in the literature [17], [50]. Since our proposed bounded functions adaptively estimate different results based on the performance evaluation of the user, assigning a constant value cannot yield an accurate weight value for each function. In other words, the movement of the user leading to a rapid and continuous change in the user's experience with different impacts from the three input parameters considered in the Weight Function. Therefore, assigning static weight settings all the time will lead to inaccurate dynamic optimization. For that, proposing an automatic function that leading to estimating the weight of each parameter automatically based on its instantaneous impact is the optimal solution. Therefore, a mathematical model is needed to automatically estimate the weight value for each bounded function. As a result, a mathematical model defined as Automatic Weight Function (AWF) is formulated in this paper to estimate the weight of each bounded function dynamically. The AWF model is evaluated as a function of the three bounded functions: $f(\gamma)$, $f(L)$, and $f(v)$. This is because the total weight of all metrics must be equal to one. Therefore, the proposed AWF model will produce a weight value of $\omega_n \in [0, 1]$ for each metric, and their total sum is equal to 1. The last AWF formula is finalized after several empirical tests have been performed to determine the validity of this proposed model. Thus, the AWF model is formulated in Eq.5:

$$\omega_n = \frac{1 - f(x_n)}{\sum_{i=1}^{F} (1 - f(x_i))} \tag{5}$$

where

- ω_n represents the weight of function n, which can be a function of γ, L, or v; therefore,$\omega_n$can be ω_γ, ω_L, or ω_v.
- $f(x_n)$ is the corresponding bounded function n that need to evaluate its weight.
- F is a metric factor that represents the total number of metrics considered for adapting HCP values. In this study, F is set to 3 since there are only three factors considered (γ, L, and v).
- $f(x_i)$ is the function of x that corresponds to i, and i varies from 1 to F. F indicates the total number of metrics used as inputs to the function $f_{WF}(\gamma, L, v)$ at Eq.1, and they are three: SINR, Load, and Speed. For simplicity, $f(x_1)$ is $f(\gamma)$, $f(x_2)$ is $f(L)$, and $f(x_3)$ is $f(v)$.

Accordingly, the AWF model (*Eq.* 5) can estimate the weight of each bounded function proposed in Eq.1. Next, Eq.1 is applied to evaluate the weight level that can be used to estimate the HCPs, as illustrated in the next sub-section.

B. DYNAMIC ESTIMATION FOR HANDOVER CONTROL PARAMETERS

This subsection demonstrates the dynamic estimation for HCPs. The estimation is individually performed for each user, based on Eq.1. That means the formula of Eq.1 will be applied to measure the three-input metrics: SINR, L, and V. Next, the output will be used to dynamically estimate the HCP settings for each individual user. The considered HCP settings in this study are two: HOM and TTT. Both will be formulated in the following two sub-subsections.

1) HANDOVER MARGIN LEVEL

The handover margin is one of the main and significant parameters used for controlling the handover decision [39], [51], [52]. This is because low and high handover margin settings may lead to a high HPPP effect and high RLF. Any inappropriate handover margin settings between low and high may also lead to similar issues. This is not satisfactory in wireless systems. The case becomes more critical with 5G networks and beyond. This is due to the use of the mm-wave, which provides very small coverage. In addition, adjusting the entire handover margin may create one of these issues as well. The entire handover margin means the handover margin setting for the cell, which means all users within the cell will use the same handover margin. Therefore, an automatic model is needed to estimate the handover margin settings for each user individually. But the adjustment of the handover margin is extremely sensitive, thus, it must be performed carefully. To achieve this target, the proposed model must define a threshold handover margin level and carefully make an adjustment around this threshold. Based on this assumption, a new model is proposed to dynamically estimate the appropriate handover margin settings for each user individually. The model consists of two parts: Part I and Part II. Part I is the threshold handover margin level which can be defined as a fixed value. Part II is the dynamic and continuous adjustment for each individual user. Thus, the total handover margin will be the summation of the fixed threshold and the adjusted part. Let us represent the threshold handover margin level as H_{thr}, and the adjusted part as (ΔM). The dynamically adjusted handover margin is mathematically represented in Eq. 6:

$$HOM = H_{thr} + \Delta M \tag{6}$$

The H_{thr} can be defined as a fixed value or it can be calculated as an average handover margin setting, $\overline{\mathcal{M}}$, which is evaluated in Eq.7:

$$H_{thr} = \overline{\mathcal{M}} = (M_{max} - M_{min}) \,/ 2 \tag{7}$$

where M_{max} and M_{min} are the maximum and minimum handover margin values. These values are assumed to be 10 dB and 0.0 dB, respectively [51], [52]. The average HOM setting can be changed in the real system. It is assumed in this simulation study to avoiding too early and too late handover probabilities. This is because the use of a very low average value will increase the too early handover occurrence, while the high average HOM values will increase the too late handover occurrence. Both cases will lead to high probabilities occurrence of HPPP and RLF, respectively.

The next part of Eq.6 is the dynamically adjusted handover margin setting, which must be carefully estimated. This is because any quick or large change in the handover margin setting may lead to an early or late handover depending on the changed direction. Thus, to avoid this issue, the change must be very smooth and scalable based on the variation of Weight Function in Eq.1. That means the adjusted level in the handover margin must be defined carefully; not too low and not too high. To control this dynamic change, the HOM threshold level is proposed as a central scale, and the dynamical change is adjusted around this level. This can be achieved by multiplying the HOM threshold level by Weight Function in Eq.1. Thus, the dynamic change in the HOM setting (ΔM) is expressed in Eq.8:

$$\Delta M = \mathcal{M} \quad f_{WF}(\gamma, L, v) \tag{8}$$

However, Eq.8 is not valid for use when the $\gamma_T < \gamma_{Thr}$ and $\gamma_S \geq \gamma_{Thr}$. This is because Eq.8 will produce a very low HOM setting in this particular condition, which may cause a very early handover. This will subsequently lead to making a handover to the wrong cell and increasing HPPP. Eq.8 is also not valid for use when the $\gamma_S < \gamma_{Thr}$ and $\gamma_T \geq \gamma_{Thr}$. This is because Eq.8 will produce a very high HOM setting in this particular condition which may lead to a very late handover that will increase the RLF. To avoid these two scenarios, the change in the HOM level (ΔM) is formulated by Eq.9 instead of Eq.8.

$$\Delta M = \begin{cases} \mathcal{M} f_{WF}(\gamma, L, v) & if\ \gamma_{T,S} \leq \gamma_{Thr} \\ \mathcal{M}\ (1 + \omega_L f(L) + \omega_v f(v)) & if\ \gamma_T < \gamma_{Thr},\ \gamma_S \geq \gamma_{Thr} \\ \mathcal{M}\ (-1 + \omega_L f(L) + \omega_v f(v)) & if\ \gamma_S < \gamma_{Thr},\ \gamma_T \geq \gamma_{Thr}. \end{cases} \tag{9}$$

Thus, the HOM level can be automatically estimated using Eq.6, which relies on Eq.7, Eq.9, and Eq.1.

2) TTT INTERVALS

Another significant HCP would be the TTT. The range of TTT intervals has been specified by 3GPP in [53], Section 6.3.5. The specified TTT (T) intervals vary from 0.00 to 5.120 seconds. However, assigning higher or lower TTT intervals may lead to a high RLF or high HPPP, respectively. Thus, the automatic adjustment based on user and network performances is the best solution that can be provided. On the other hand, adjusting the TTT for the entire system (all users in the cell) may lead to critical issues for some users since they have different experiences. Some users may have the worst experiences at cell boundaries, while others may have good experiences. Thus, the best solution is to individually adjust the TTT for each user. The adjustment must be carefully performed. Therefore, we propose to adjust the TTT up or down by adding or reducing the threshold TTT with a specific interval defined as ρ. The performed adjustment is based on the variation of f_{WF} in Eq.1. In case the f_{WPF} increases, the TTT will be increased by ρ interval of time. On the other hand, if the f_{WF} decreases, the TTT will be decreased by ρ interval of time. The instantaneous f_{WPF} level is usually compared to the previous f_{WPF} record. In order to avoid unnecessary adjustment of TTT, we defined the threshold level for the f_{WF} variation as φ. If the instantaneous f_{WF} is greater than the previous f_{WF} record by φ level, the system can perform the adjustment, otherwise, no adjustment can be done. This is mathematically represented in Eq.10.

$$AT = \begin{cases} T - \rho & if\ f_{WF} \leq f_{WF} + \mathcal{Q} \\ T + \rho & if\ f_{WF} \geq f_{WF} + \mathcal{Q} \end{cases} \tag{10}$$

where,

AT	The instantaneously adjusted TTT
T	The threshold TTT level, initially defined as a fixed proper interval, then T willbe equal to AT in the second adjustment and onwards
$\mathcal{Q}$	level of optimization step
ρ	level of optimization interval

However, Eq.10 cannot be implemented in two cases. The first case is when the T reaches Zero. The TTT cannot be negative (it cannot go below the minimum TTT level defined by 3GPP). The second case is when the T reaches the maximum TTT defined by 3GPP. A specific formula must be devised for each of these two special cases. For the first case, the TTT cannot be adjusted up; while for the second case, the TTT cannot be adjusted down. Thus, for these two cases, the adjusted TTT is formulated by Eq.11 and Eq.12, respectively.

$$AT_{min} = \begin{cases} T & if\ f_{WF} \leq f_{WF} + \mathcal{Q} \\ T + \rho & if\ f_{WF} \geq f_{WF} + \mathcal{Q} \end{cases} \tag{11}$$

And

$$AT_{max} = \begin{cases} T - \rho & if\ f_{WF} \leq f_{WF} + \mathcal{Q} \\ T & if\ f_{WF} \geq f_{WF} + \mathcal{Q} \end{cases} \tag{12}$$

From Eq.10 to Eq.12, the TTT interval can be dynamically adjusted based on the variation of Weight Function in Eq.1. Accordingly, the adaptive TTT (ΔT) intervals can be determined by Eq.13:

$$\Delta T = \begin{cases} AT & if\ T_{min} < T < T_{max} \\ AT_{min} & if\ T = T_{min} \\ AT_{max} & if\ T = T_{max} \end{cases} \tag{13}$$

The constants, ρ and $\mathcal{Q}$, are meant to adjust the resolution in which the TTT intervals are updated. If these constants are selected to be small, higher resolution of TTT is achieved. However, if too high, the TTT resolution may impose high computational complexity and delays to the system. Thus, for simplicity, the values of ρ and $\mathcal{Q}$ are selected to be 0.04 s and 0.1s throughout the simulation. It can be further noticed that when the updated value is saturated at T_{max} or T_{min}, no further updates are considered. The T_{max} or T_{min}, are determined from the 3GPP recommendations as 0.0 sand 5.12s, respectively. The initial value of TTT for all implemented HPSO algorithms is assumed to be 100 milliseconds.

IV. SYSTEM AND SIMULATION MODELS

The simulation model of this study is developed to simulate the real 5G network. The network is modeled according to LTE-Advanced Pro 3GPP Rel.16 specifications that are explained by 3GPP in [2]–[8], [46], [50]. The network is deployed by considering several small hexagonal cell layout models, parts of which are illustrated in Figure 3. The number of hexagonal cells can be automatically increased based on the simulation time interval defined in the simulation. Each hexagonal cell is built with an inter-site distance of cell radius R (in meter) and one eNB located at its center, as illustrated in Figure 3. Each hexagonal cell also consists of three sector antennas. As for frequency planning, a unity frequency reuse factor is assumed for all cells.

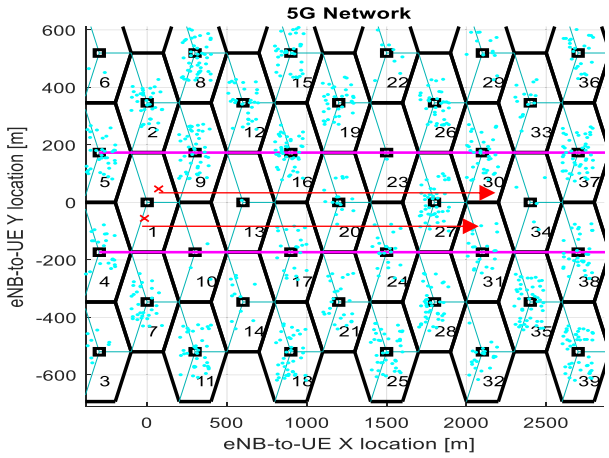

FIGURE 3. System model with several hexagonal cells, each consist of three sectors.

In each hexagonal cell, a number of mobile users are generated with random coordinates within the cell hexagonal boundaries. Initially, 200 users are generated and randomly distributed inside each hexagonal cell. Throughout the simulation cycles, the number of users is randomly and periodically changed in each cell. That means the load traffic for each eNB is automatically and periodically changed from time to time to represent the real network environment. This is considered in the developed simulation model so as to mimic a random generation of load traffic throughout the simulation and to fully enable the admission control functionality at the target cell through the mobility of users. Each user is equipped with an Omni-directional antenna to communicate with the serving network.

The radiation pattern of each antenna matches those described by 3GPP in [50], [54]–[56], and it is mathematically exemplified as:

$$A(\theta) = -min\left[12\left(\frac{\theta}{\theta_{3dB}}\right)^2, A_m\right] \quad where -180 \le \theta \le 180 \tag{14}$$

where, $A(\theta)$ exemplifies the gain of antenna (dBi) in the direction of θ, which is the angle among the steering direction of the antenna and the direction of interest; θ_{3dB} denotes the 3dB beam width which corresponds to 65 degrees; and A_m denotes the maximum attenuation which corresponds to 20 dB ($A_m = 20\ dB$) with three sectors in each cell.

Six different user speeds are considered during the simulation study. The considered speeds range between 40 km/hour and 140 km/hour. These speeds are applied to assess the influence of different mobile speeds on network performance. They represent the characteristics of vehicle speeds in urban and suburban areas and are therefore accepted for theoretical investigations. The specific mobile speeds considered in the simulation are presented in Table 1.

A Directional Mobility Model (DMM) is proposed for all measured mobile users throughout the network. Mobile users are allowed to move in only one direction with the range of [0°], as illustrated in Figure 3. The measured users are initially generated in the cell that is numbered one in Figure 3. Next, the users only move in one direction between the solid pink lines, as illustrated in Figure 3. Since users are initially generated at random coordinates, their movements will be in different parallel paths to each other. That means all users will move parallel to each other in one direction. That will enable us to consider additional and diverse handover scenarios and probabilities since users are moving parallel over different paths within the cells. This will further increase the accuracy of results as well. The users' movements are periodically updated in the simulation. The periodical interval is identified as 50 ms. The movement distance is matched with the periodical interval.

In this study, 15 users are chosen to investigate the performance of the proposed algorithm so as to compare with other algorithms from the literature. The 15 users are randomly generated inside cell#1 in the first simulation cycle. Therefore, each user initially has a different coordinate in the cell. Since the mobility of users is directed to one direction, each user has a different path that is parallel to the other measured users. Next, the performances of the 15 users are measured in every simulation cycle (which is 50 ms) during their mobility within the cells. The measurement was conducted to illustrate the performance of wireless networks based on different HPSO algorithms. The average values of RSRP, HOP, HPPP, and RLF are calculated in every

TABLE 1. System and simulation parameters [38], [50]–[52], [57].

Network Parameter	Assumption
Environment	Micro cells, Urban areas, 5G Rel.16System
Cellular Layout	Hexagonal grid,
No. of Hexagonal Cells	Dynamically changed based on simulation time
No. of Sectors per cell	3 Sectors
Interference Model	Co-Channel Interference (CCI) from the first tier
Path Loss Model	$L = 58.8 + 37.6\ x\ log_{10}(d) + 21\ log_{10}(f_c)$
Shadow Fading Model	Gaussian-distributed random variable with zero mean and σ_{dB} standard deviation in dB [57, 58]
Fast Fading Model	Rayleigh fading model [59]
eNBs antenna height	15 m
Cell radius(d)	200m
Carrier frequency	28 GHz
Total eNB TX Power	46 dBm
Shadowing (σ)	8 dB
White Noise Power Density (Nt)	-174 dBm/Hz.
eNBs Noise Figure	5 dB
Thermal Noise Power (Np)	Np = Nt + 10 log (BW x106) dB
Number of tested UEs	15 UEs distributed initially randomly at Cell#1
UE Noise Figure	9 dB
UE height	1.5 m
UE's Antenna Gain	0 dB
UE's Antenna	1 (Omni-directional)
Mobility Model	DMM
UE's speeds	Ranging from 40 to 140 km/hour in steps of 20 km/hour
Resource Distribution	evenly over all the active UEs
System Bandwidth	500 MHz
Cyclic Prefix length	Normal
Number of PRBs	2500 PRBs
Modulation Scheme	AMC scheme
Resource Distribution	evenly over all the active UEs
HO Decision Algorithm	$RSRP_S > RSRP_T + HOM$
Q_rxlevmin	-101.5 dBm
Handover Margin	Adaptive
TTT	Adaptive (0 ms to 5120 ms)
T311 interval	10 s

No.: Number
Q_rxlevmin: Minimum required RX level in the cell (dBm) [3GPP TS 36.304]

simulation cycle. Thus, the presented results are the average values for all 15 users.

The simulation commenced based on previous illustrated settings. It began with identifying the required network parameters, followed by building the entire simulated network environment. Next came the mobility model. During simulation, the users' directions and positions are periodically updated, and their Euclidian distances from the eNB in the network are calculated in a distance matrix. From this distance matrix, the experienced path losses on the signal are estimated in addition to the log-normal shadowing and Rayleigh fading in multipath scenarios. The RSRP and SINR perceived by each UE are then calculated over each carrier received signals. Each eNB in the network updates the RLF and Ping-Pong report during the simulation. Moreover, the eNB updates the load report and transmits its load information to another eNB in the network. From the perspective of the UE, the average SINR and RSRP over the carrier is measured by each UE and then transmitted to the respective eNB for the optimization process. The eNB performs the Modulation and Coding Scheme (MCS) selection according to the received SINR and RSRP reports, as illustrated in Table 2. The self-optimization process is then executed.

TABLE 2. MCS in LTE-advanced system [60].

CQI index	MCSs	MSs	Coding Rate	SINR Threshold [dB]
1	MCS-01	QPSK	1/8	- 6.5
2	MCS-02	QPSK	1/5	- 4.2
3	MCS-03	QPSK	1/4	- 3.5
4	MCS-04	QPSK	1/3	- 1.5
5	MCS-05	QPSK	1/2	0.5
6	MCS-06	QPSK	2/3	2.0
7	MCS-07	QPSK	4/5	4.5
8	MCS-08	QPSK	1/2	6.1
9	MCS-09	16-QAM	2/3	8.1
10	MCS-10	16-QAM	4/5	10.9
11	MCS-11	16-QAM	2/3	12.5
12	MCS-12	64-QAM	3/4	13.5
13	MCS-13	64-QAM	4/5	16.0

Upon the completion of the self-optimization process, the serving eNB performs the handover decision according to the Measurement Report (MR) and estimated HCPs by executing the handover procedure sequence in 3GPP [51], [52]. If the serving eNB provides satisfactory signal quality, the connection with the UE will be maintained.

The radio link connection condition is regularly monitored and updated in the serving eNB. In the case of RLF detection, the Radio Resource Control (RRC) re-establishment procedure will be initiated. In this procedure, the UE scans the received signals from all neighboring cells, and then selects the target cell that can fulfill the minimum required signal level. The UE will select the cell that provides the strongest signal quality (if multiple cells satisfy the criteria). Upon the selection of the cell by the UE, the RRC re-establishment procedure is initiated to configure the connection within T311 interval. Conversely, if none of the cells satisfy the minimum requirements, the Non-Access Stratum (NAS) recovery procedure is enabled. The UE continues to identify a suitable cell in the target eNB throughout the NAS recovery procedure. The search is repeated until a suitable cell is identified and reconnection takes place. Finally, the system performance is evaluated at the end of each simulation cycle.

The simulation model is used to investigate various handover self-optimization algorithms from the literature. It also implemented the developed algorithm to validate its performance in the system. The simulation's performance results for the developed algorithm are then analyzed and compared to the performance of various HPSO algorithms with different mobile speeds. The essential 5G parameters defined in the 3GPP specifications (Rel.16) are considered in this simulation, as listed in Table 1.

V. KEY PERFORMANCE INDICATORS

Four Key Performance Indicators (KPIs) are used to evaluate network performance. The KPIs have been selected due to their significance. They are main criteria usually used in evaluating wireless network performance during user mobility. The four KPIs are explained below:

- ***RSRP:*** Received Signal Strength has been defined by 3GPP in LTE/LTE-Advanced as a RSRP. It is a significant KPI that is usually employed for measuring wireless network performance during user mobility. This is due to the rapid changes in the received RSRP level during the movement of users within the cells. Also, it is the main factor that has a direct impact on the total system performance in terms of SINR, throughput, and outage probability.
- ***HOP:*** HOP is the Handover Probability (sometimes presented as a handover rate) that may occurs during user mobility. It is a significant KPI that is usually used for evaluating wireless network performance during the mobility of users within the cells. This is because the mobility of users can lead to a rapid change in the received signal strength, prompting the need for switching connection handover) from one cell to another so as to provide better service. The communication link switches from an old BS to a new one that provides better continuous signal with enough bandwidth. This handover rate can be changed with the implementation of different ***HPSO*** algorithms. Therefore, HOP is the main indicator for studying the performances of different ***HPSO*** used.
- ***HPPP:*** HPPP, Handover Ping-Pong Probability, is the probability of unnecessary handover that can result through the mobility of users. This may occur due to various reasons such as unsuitable settings in the HCP settings or inaccurate handover decision. If this case arises during user mobility, it leads to an unstable connection with bad communication quality. Since this is a critical issue in wireless networks, the HPPP becomes one of the main KPIs that are usually used for evaluating wireless network performance during the mobility of users within the cells. Therefore, it is considered in this study.
- ***RLF:*** The RLF, Radio Link Failure, is recorded communication dropping rate during user mobility due to a deterioration in the RSRP level. It is recorded when the serving RSRP goes below a specific threshold level before the mobile switches the connection to a new BS. The threshold level is usually defined by a standard which differs from one system to another. It is considered as a significant KPI that are commonly used to calculate the performance of wireless networks throughout user mobility. This is because the mobility of users can lead to a rapid change in the received signal strength. This may cause a call to get dropped before the connection switches to a new cell due to poor signal quality or no resources available (in some cases). This issue sometimes occurs due to unsuitable settings in the HCP settings or incompatible handover decision algorithm. Thus, RLF is a necessary KPI that should be considered for evaluating wireless network performance during user mobility.

Based on these performance indicators, the results are presented and discussed in the next section.

VI. RESULTS AND DISCUSSION

This section presents the collected results from the simulation study. The performance results of the proposed algorithm are discussed and later and compared to three other algorithms selected from the literature. All considered algorithms have been investigated with six different mobile speed scenarios to illustrate their performance in various conditions. The algorithms are assessed and validated based on simulations using the 5G network. All presented results are average values taken from the15 users considered in the measurements. Performances are independently measured for each user in every simulation cycle (which is 50 ms). Next, the average value is taken over all measured users in every simulation cycle. Thus, the presented results are the average values over all 15 users.

The results of the proposed algorithm are compared to the HPSO based on distance (Dis) [2]–[8], WPHPO (labeled as HPI in the figures)[17], and FLC [15] algorithms. The Dis, HPI, and FLC algorithms are chosen from the literature since they mostly focus on developing the HPSO function. They are also clearly explained as compared to other algorithms. Accordingly, the presented results illustrate the effect of the developed algorithm on the RSRP, HOP, HPPP effect, and RLF. Based on these KPIs, the results are presented and discussed in four subsections, as illustrated in the following.

A. REFERENCE SIGNAL RECEIVED POWER (RSRP)

In this subsection, the results of the received signal strength (RSRP) are presented and discussed. Figure 4 displays the RSRP in the form of Cumulative Distribution Function (CDF) as the average for all measured users. The presented results demonstrate the performance of various automatic self-optimization algorithms with different mobility speed scenarios. The results also indicate that there is no specific algorithm that can provide the highest RSRP level with all mobile speed scenarios. For 40 kmph, 60kmph, and 80kmph, no significant improvement was achieved by the proposed algorithm as compared to the benchmark algorithms. For the highest mobile speed scenarios (100-140 kmph) the

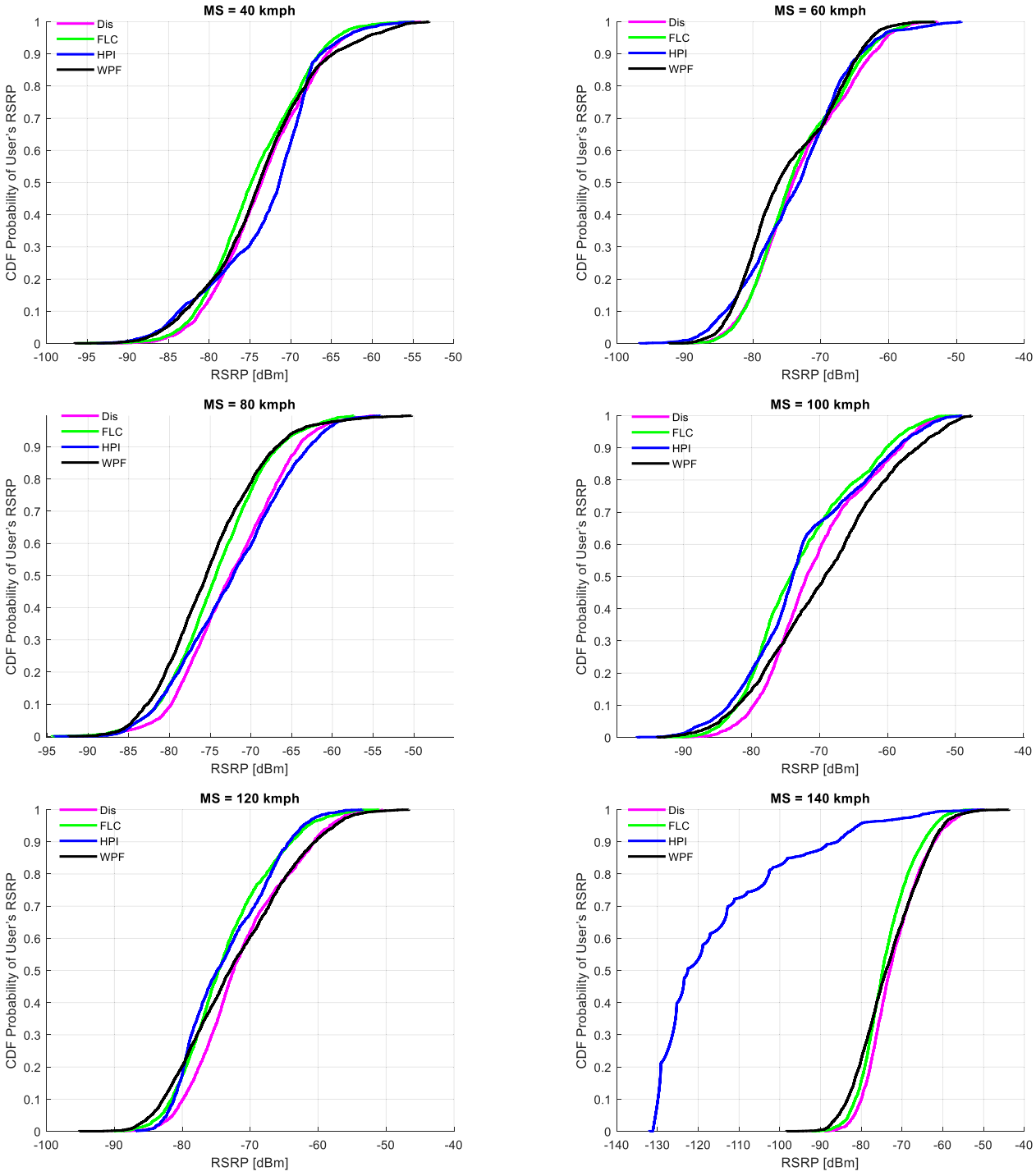

FIGURE 4. Average CDF of RSRP with various mobile speed scenarios.

proposed algorithm and the Dis algorithm provide noticeable enhancements compared to the benchmark algorithms. However, the mean values of the enhancements are not so high, especially if the HPI algorithm is ignored due to its - worst performance for 140 kmph. The mean variations between the performances of various algorithms range between 2.3 dBm to 4.6 dBm without considering the HPI algorithm for 140 kmph. If HPI is considered, the exact mean variations between the minimum and maximum levels are 3.4 dBm, 3.3 dBm, 3.3 dBm, 4.6 dBm, 2.3 dBm, and 49 dBm for 40 kmph, 60 kmph, 80 kmph, 100 kmph, 120 kmph, and 140 kmph, respectively. The HPI provides the worst results

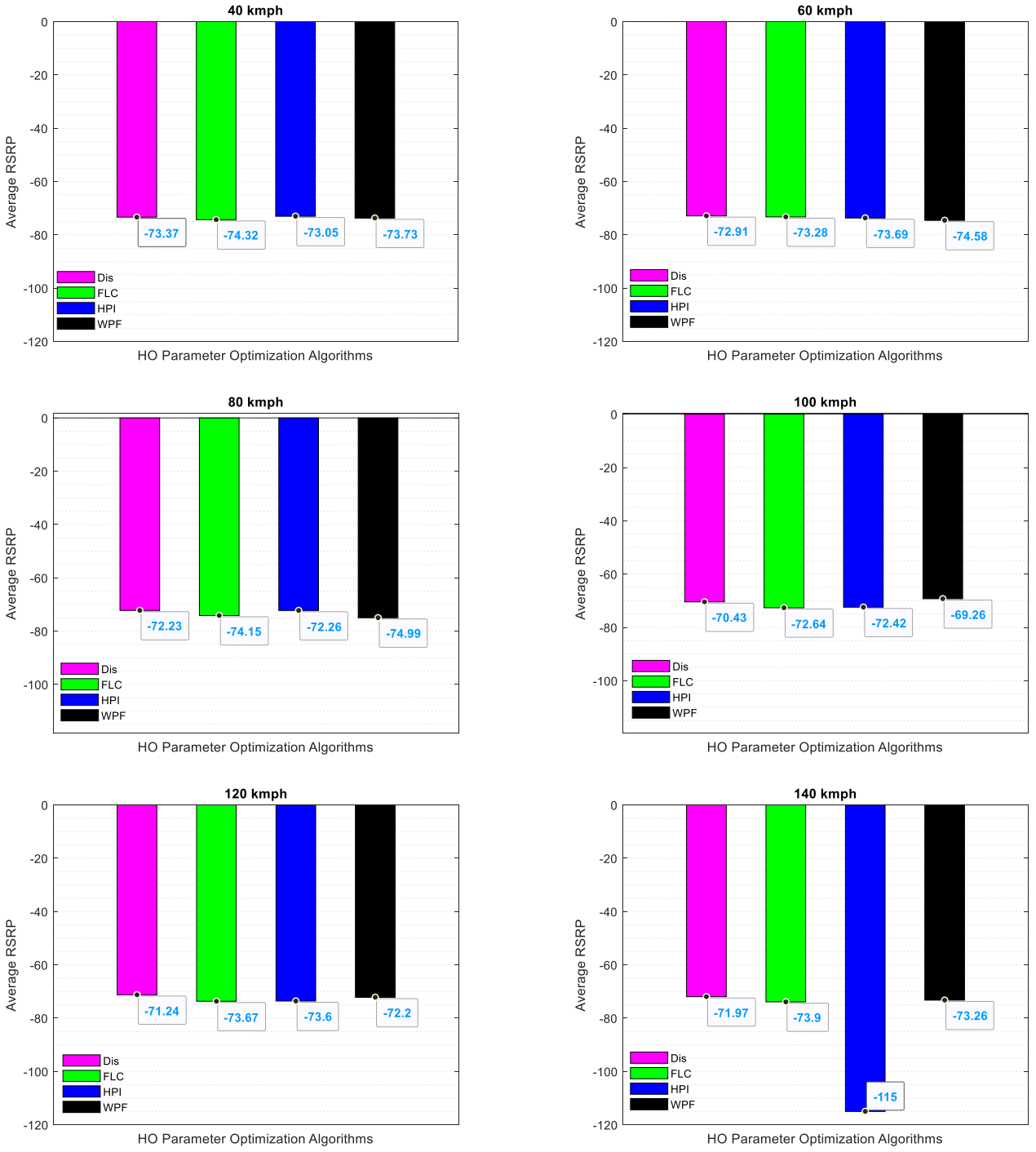

FIGURE 5. Average RSRP overall simulation time with various mobile speed scenarios.

for 140 kmph. Therefore, if the HPI is ignored, reasonable results and small differences are achieved. It can be further noted that the Dis, FLC, and the proposed algorithm have achieved very similar RSRP results with only a small variation. The differences between the mean performances attained by these three algorithms are 1.3 dBm, 2.4 dBm, 3.3 dBm, 4.6 dBm, 2.3 dBm, and 1.7 dBm for 40 kmph, 60 kmph, 80 kmph, 100 kmph, 120 kmph, 140 kmph, respectively.

Figure 5 presents the average RSRP over all measured users and over all simulation times for each independent mobile speed scenario. The results indicate that the minimum

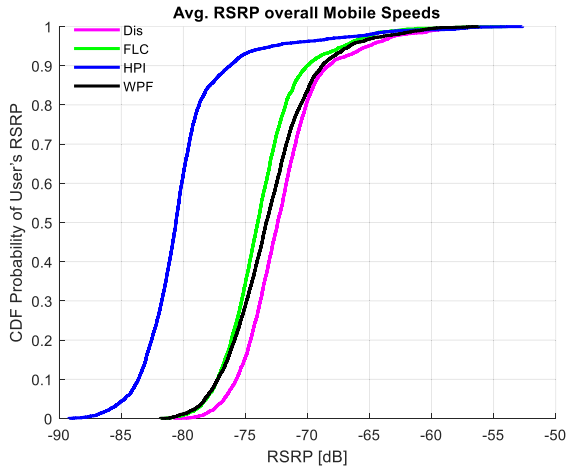

(a) Average CDF overall mobile speed scenarios

(b) Final Average overall mobile speed scenarios

FIGURE 6. Average RSRP overall mobile speed scenarios.

achieved RSRP level is greater than -75dBm for all the algorithms with all mobile speed scenarios, except HPI with 140 kmph. The results further demonstrate the performance of the proposed algorithm in comparison to other algorithms. In the case of lower mobile speed scenarios (40kmph, 60kmph, and 80kmph), the proposed algorithm provides a lower RSRP level with an average of 1.7 dBm. However, in the case of higher mobile speed scenarios (100 kmph, 120 kmph, and 140 kmph), the proposed algorithm produces better results than HPI and FLC. It outperforms the Dis, FLC, and HIP algorithms for the mobile speed of 100 kmph by 1.15dBm, 3.4dBm, and 3.15dBm, respectively. Moreover, it outperforms the FLC and HIP algorithms for 120 kmph by -1.45 dBm and 1.4 dBm, respectively. In the case of140 kmph, the proposed algorithm outperformed the FLC and HIP algorithms by 31.7 dBm and 0.6 dBm, respectively. Even when it was less than the Dis algorithm (with 120 kmph and 140 kmph), it was only lower by around 1 dBm.

Figure 6 presents the average RSRP over all measured users and over all mobile speed scenarios. The results in Figure 6 (a) illustrate the average RSRP over all measured users and over all mobile speed scenarios in the form of CDF. While Figure 6 (b) presents the average RSRP over all measured users taken over all simulation times and then taken over all mobile speed scenarios. Both Figures demonstrate that the proposed algorithm provides noticeable enhancements, especially when compared to HPI and FLC. Even though it was lower than the Dis algorithm, it was only lower by 1 dBm. Nevertheless, the performance of the proposed algorithm is better than the Dis algorithm based on the other KPIs, as will be seen later.

These results provide two indications. First, the Dis, FLC, and the proposed algorithm can be considered as candidate algorithms for the 5G network, yet further investigations are needed before recommendations. Second, the proposed algorithm presented noticeable achievements, making it a promising solution as long as its performance is noticeable based on the other KPIs.

B. HANDOVER PROBABILITY (HOP)

Figures 7 and 8 present the average handover probability results based on the considered algorithms. In Figure 7, the handover probability is presented as the average rate over all measured users with various mobile speed scenarios. While in Figure 8, the handover probability is presented as an average rate over all measured users and over all mobile speed scenarios. The results generally indicate that at the initial operation period, the handover probability is high. This is more apparent for lower mobile speed scenarios below 100 kmph and for the average handover probability over all mobile speed scenarios (Figure 8 (b)). This phenomenon occurs because the network operation begins in accordance with the initially defined HCP settings. After a while, the HCP settings are automatically optimized and updated by the considered algorithms. That leads to a different impact on the handover probability which varies based on the reaction and robustness of the operating optimization algorithm. The proposed and HPI algorithm have shown that they react more with mobile speed scenarios and optimizations updated with time. However, the performances of Dis and FLC did not present significant reactions with different mobile speed scenarios or even with optimizations updated with time. This is usually due to the robustness design of the optimization algorithm.

In Figure 7, the results demonstrate that the proposed algorithm with the mobile speed below 100 kmph produces lower handover probability, which is further reduced with time. However, with mobile speed scenarios equal to or above 100 kmph, the proposed algorithm produced changeable handover probabilities that rapidly fluctuate with time. In Figure 8, the results show that the proposed algorithm provides a noticeable reduction gain in the handover rate,

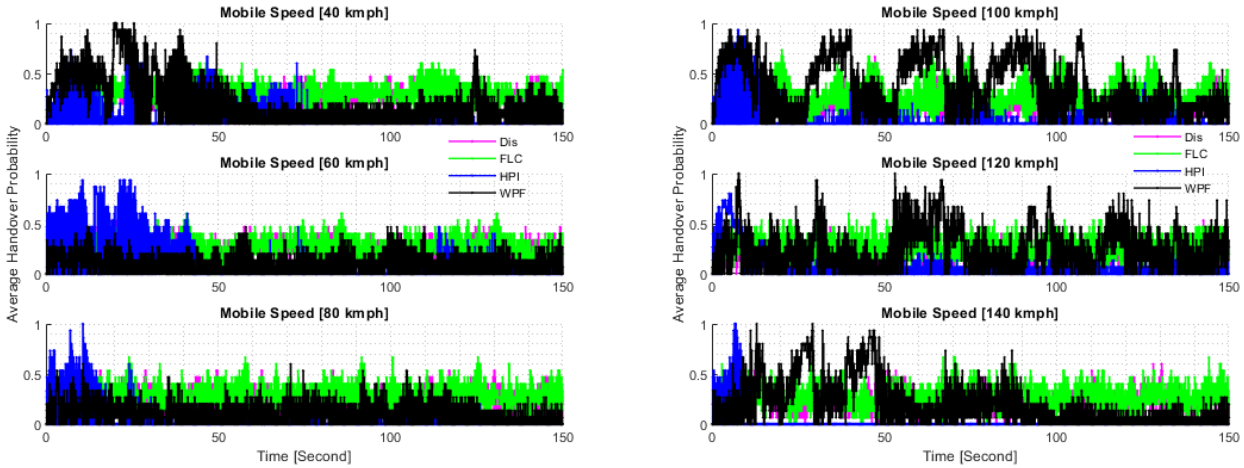

FIGURE 7. Average handover probability overall mobile measured users versus time with various mobile speed scenarios.

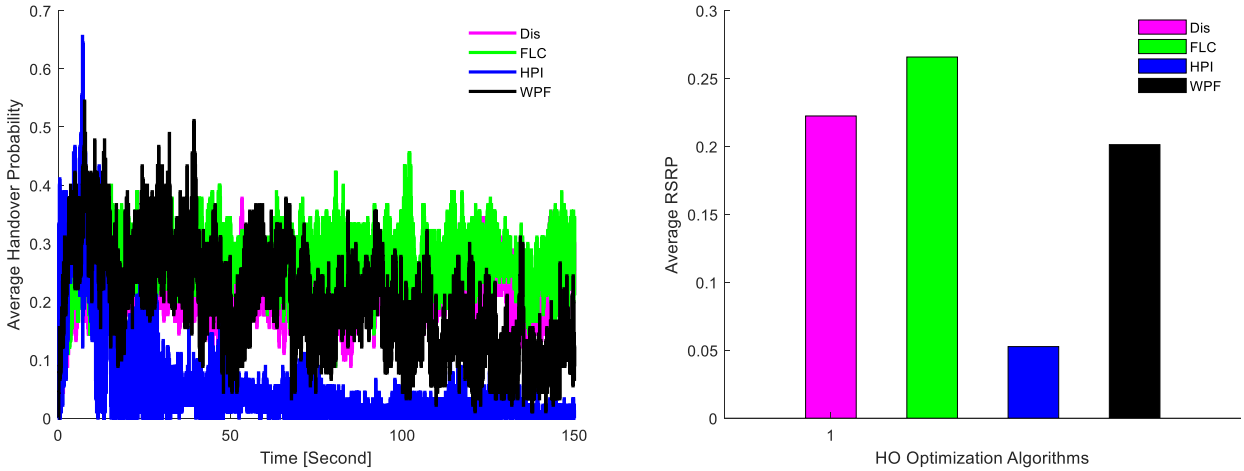

(a) Average HO rate overall mobile speed scenarios

(b) Final Average HO rate overall mobile speed scenarios

FIGURE 8. Average handover probability overall mobile speed scenarios versus time.

especially when compared to the Dis and FLC algorithms. The HPI still offers the lowest average handover rate over all mobile speed scenarios. Accordingly, the average reduction gains achieved by the proposed algorithm are around 9% and 24% lower than the Dis and FLC algorithms, respectively. However, the highest or the lowest handover probability is not always considered as bad or good indicators. The most significant performance indicators are the Ping-Pong effect and RLF, which will be discussed in the next two subsections.

C. HANDOVER PING-PONG PROBABILITY (HPPP)

The handover Ping-Pong probability is the unnecessary handover that may occur due to suboptimal HCP settings. Suboptimal HCP settings can be statically defined or automatically estimated. In the static case, HPPP occurs if the HCP settings are manually defined at minimum levels. In the automatic case, HPPP occurs if inappropriate HCP - settings are estimated by an automatic HPSO algorithm. In both cases, the suboptimal HCP settings that cause HPPP usually take place when the HCP settings are at minimum levels. That leads to early handover before it is needed. This, in turn, may lead to increased HPPP in some situations, especially for mobile users located at the cell edges. Moreover, the increase in mobile speeds further increases the HPPP probability. This, in turn, increases network resource wastage and degrades network performance. Therefore, HPPP should be reduced as much as possible to preserve network resources.

Figures 9 and 10 present the average handover Ping-Pong probability results based on the different algorithms considered. In Figure 9, the HPPPs are presented as the average rate over all measured users with various mobile speed scenarios. While in Figure 10, the HPPPs are presented as the average rate over all measured users and over all mobile speed scenarios. Similar to the handover probability, the results show that at the initial operation period, the HPPPs are high. The case is more apparent with lower

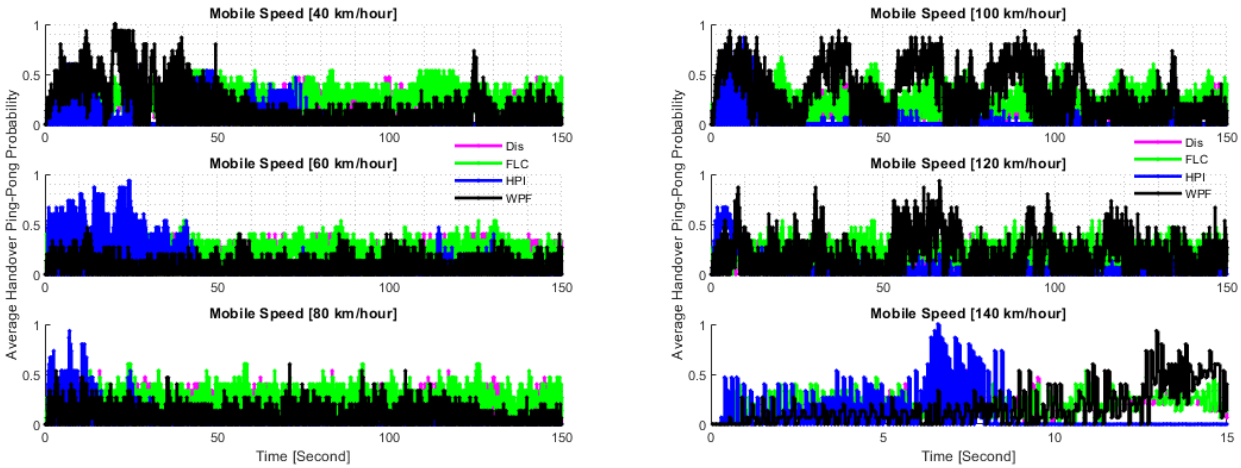

FIGURE 9. Handover Ping-pong probability versus Time with different mobile speed scenarios.

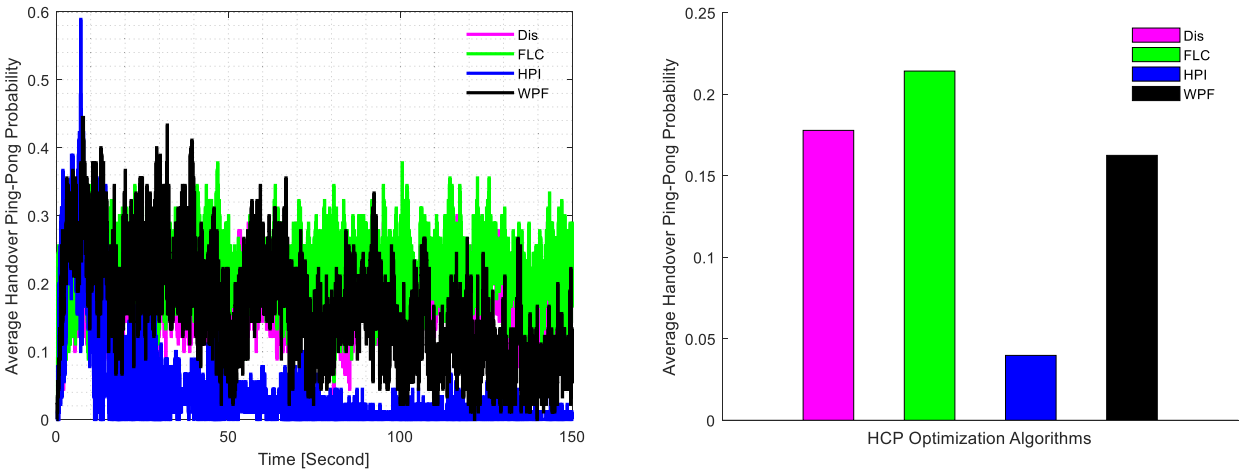

(a) Average HPPP rate overall mobile speed scenarios

(b) Final Average HPPP rate overall mobile speed scenarios

FIGURE 10. Average handover ping-pong probability over all mobile speed scenarios versus time.

mobile speed scenarios below 100 kmph as well as with the average HPPP probability over all mobile speed scenarios (Figure 10 (b)). The occurrence of this phenomenon can be explained using the same justification mentioned in the previous subsection. The results further indicate that the proposed algorithm and the HPI algorithm react more with mobile speed scenarios and optimizations updated with time. However, the performances of Dis and FLC did not present significant reactions with different mobile speed scenarios or with optimizations updated with time.

In Figure 9, the results indicate that the proposed algorithm with mobile speeds below 100 kmph produces lower HPPP compared to the Dis and FLC algorithms. However, when the mobile speed scenarios are equal to or above 100 kmph, the proposed algorithm produces changeable handover probability that rapidly fluctuates with time. In Figure 10, the results show that the proposed algorithm provides a noticeable reduction gain in the HPPP rate, especially when compared to the Dis and FLC algorithms. The HPI still offers the lowest handover rate regarding the average over all mobile speed scenarios, but this is not a good indication for HPI (as illustrated in the next subsection). Accordingly, the average reduction gains achieved by the proposed algorithm are around 9% and 24% lower than the Dis and FLC algorithms, respectively. However, the lowest HPPP rate can sometimes be considered as a bad indicator. This is because there is a tradeoff between the HPPP and RLF, which is further explained in the following subsections.

D. RADIO LINK FAILURE (RLF)

The RLF is another significant indicator for evaluating network performance. Similar to the HPPP with a different direction, the suboptimal HCP settings can be statically defined or automatically estimated. In the static case, the RLF occurs if the HCP settings are manually defined at maximum levels. In the automatic case, the RLF occurs if inappropriate

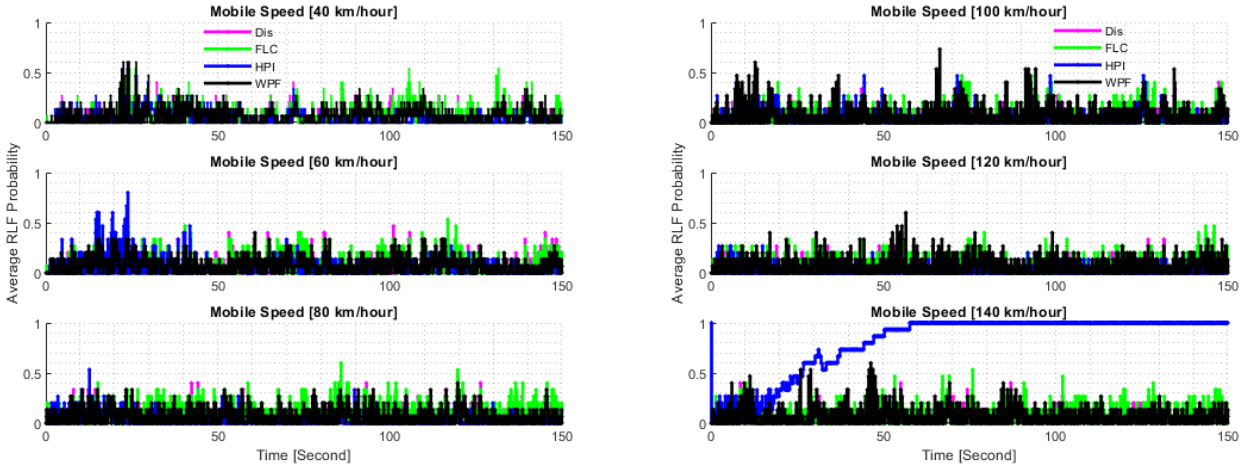

FIGURE 11. Handover RLF versus Time with different mobile speed scenarios.

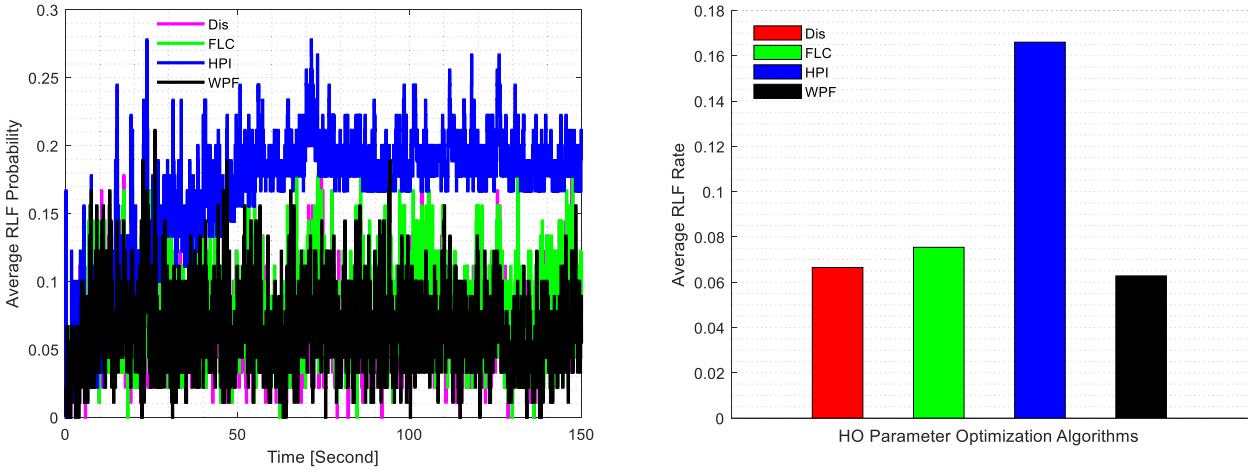

FIGURE 12. Average RLF over all mobile speed scenarios versus time.

HCP settings are estimated by an automatic HPSO algorithm. In both cases, the suboptimal HCP settings that cause RLF usually happen when the HCP settings are at maximum levels. That leads to late handover which may subsequently lead to increased RLF in some situations, especially for mobile users located at cell edges or those moving with high mobile speeds. This, in turn, will increase network resources wastage and degrade network performance. Therefore, RLF should be reduced as much as possible to preserve network resources.

Figures 11 and 12 present the average RLF probability recorded based on the different algorithms considered. In Figure 11, the RLFs are presented as the average rate over all measured users with various mobile speed scenarios. While in Figure 12, the RLFs are presented as an average rate over all measured users and mobile speed scenarios. The results generally indicate that the RLFs are changeable with time for all mobile speed scenarios. The results further reveal that all algorithms continuously react with time.

In Figure 11, the results indicate that there are no clear differences between these algorithms. However, in Figure 12, the proposed algorithm presents a noticeable reduction gain in the RLF rate compared to the other algorithms. The HPI causes the highest RLF rate as an average over all mobile speed scenarios. Accordingly, the average reduction gains achieved by the proposed algorithm are around 6%, 17%, and 62% lower than the Dis, FLC, and HPI algorithms, respectively. This is a significant achievement reached by the proposed algorithm.

E. DISCUSSION

In previous subsections, the performances of different algorithms are discussed based on four KPIs. The results show that a tradeoff is present between the performances achieved due to the different KPIs.

It can be stated that the RSRP levels achieved by the Dis, FLC, and the proposed algorithm are above the

acceptable level by more than 26.15dBm, the considered threshold level in the 5G system is around −120 dBm. On the other hand, the HPI algorithm provided lower results (below −101.5dBm), specifically with 140 kmph. The proposed algorithm also offers the best results compared to the HPI and FLC algorithms. The Dis algorithm is better than the proposed algorithm, but the difference is only by 1 dBm. Thus, the presented results indicate that the Dis, FLC, and the proposed algorithm have the capability to support stable communication in 5G networks, making them suitable for implementation in 5G networks. However, this does not mean that they are all efficient for use in 5G networks without further investigations that consider more scenarios and KPIs. These results also indicate that the final conclusion should be stated based on the performance of Dis, FLC, and the proposed algorithms, while primarily ignoring the performance of the HPI algorithm.

According to the handover probability, the proposed algorithm (concerning the final average over all users, mobile speed scenarios, and simulation times) achieved a lower rate than the Dis and FLC algorithms. The HPI still attained an even lower rate than the proposed algorithm, but it has an issue regarding the RSRP and RLF performances. Offering lower handover rate is not always a good indication. This is because with the implementation of handover parameters self-optimization algorithms, the impact of HCPs in reducing the handover probability can be due to two main reasons. First, the high-level selection in the HCP settings leads to delayed handover. This, in turn, leads to an increase in RLF, which is a bad indicator. Second, the implementation of efficient handover parameters self-optimization algorithm leads to the selection of optimal HCP settings. This usually leads to improved network performance in general. Therefore, it can be noted that even the proposed algorithm contributes to reducing the handover rate, but the reduction in handover rate is not always considered as an advantage. Thus, the HPPP and RLF must be investigated to establish a final conclusion.

For the handover Ping-Pong rate, the proposed algorithm performed lower than the Dis and FLC algorithms in the final average. The HPI also performed lower than the proposed algorithm, but it has an issue concerning the RSRP and RLF performances, as previously illustrated. Offering a lower handover Ping-Pong rate is not always a good indication. This is because the utilization of higher HCP settings leads to a reduction in the HPPP rate. This simultaneously leads to delayed handover which, in turn, leads to an increase in RLF. However, a reduction in the HPPP rate is sometimes a good indication. This is due to the use of efficient handover parameters self-optimization algorithms that estimate the optimal HCP settings. The proposed algorithm contributes to reducing the handover Ping-Pong rate, yet that reduction is not always considered as an advantage. The tradeoff between HPPP and RLF illustrates the performance more clearly.

For the RLF rate, the proposed algorithm performed lower in the final average compared to the Dis, FLC, and HPI algorithms. However, a reduction in the RLF rate is not always a good sign. This is because the utilization of lower HCP settings leads to a reduction in the RLF rate. This will simultaneously lead to early handover which, in turn, causes an increase in HPPP. Sometimes, the reduction in the RLF rate is a good indication as it is due to the use of efficient handover parameters self-optimization algorithms that estimate the optimal HCP settings. Thus, the final conclusion should be stated based on the tradeoff performance between HPPP and RLF.

The presented results show that, the proposed algorithm provides noticeable enhancements on average compared to other algorithms. As previously illustrated, the proposed algorithm provides distinct improvements in terms of RSRP, HOP and HPPP compared to the Dis and FLC algorithms. The HIP algorithm offered lower HOP and HPPP compared to the proposed algorithm, but its RLF was significantly higher. That means the tradeoff between HPPP and RLF achieved by the proposed algorithm is better than what is achieved by the HPI. Moreover, the proposed algorithm provides noticeable enhancements in terms of RLF when compared to all algorithms. This indicates that the proposed algorithm contributes to significant improvements in comparison to other investigated algorithms.

These enhancement gains also lead to considerable advancements in network performance with different mobile speed scenarios. They reinforce system performance by increasing connection continuity and reliability, especially through high mobility speeds. They ensure that the radio link connection will be maintained between the served UE and the serving network. This leads to a seamless connection, making it reliable through the mobility of the UE within the cells. Accordingly, the results demonstrate that the proposed algorithm achieves higher gains than all other algorithms with different mobile speed scenarios. Thus, the proposed algorithm provides the best reduction gains when compared to other algorithms. This is attributed to the robustness of the proposed algorithm in estimating suitable HCP values.

These enhancement gains are attributed to the influences of three considered factors (SINR, UE's speed, cell load) and the individual estimation for each UE. The proposed algorithm independently performs the optimization for each UE based on the UE's SINR, speed, and cell loads. This leads to the estimation of suitable HCP values for each UE, independently, without affecting other UEs in the cell. It allowed the UE to connect to the best cell continuity without any retraction from the serving network, which means that the proposed algorithm discharges the central control in the optimization process. On the other hand, the other algorithms from previous works performed the optimization process centrally by the eNB. This central control causes restriction to the UEs. This adjustment is useful for some UEs, but can simultaneously affect others. The proposed algorithm is more robust than the existing algorithms in the literature. Thus, the proposed algorithm can be considered as one of the robust HPSO algorithms for 5G systems.

VII. FUTURE DIRECTIONS

Handover Parameter Self-Optimization is one of the significant functions that have been introduced in 4G and 5G networks to automatically optimize HCPs. The automatic self-optimization operations characteristic will enable this technology to be part of Sixth Generation (6G) mobile networks with further improvements as well. Also, some new technology will be introduced and other factors will be used. In this section will give a brief and general guidance for future works that need to be conducted in future.

- **Mobility with the integration of 6G and satellite networks:**The integration between 6G and satellite technologies will be one of the targets that need to be achieved in future wireless networks [61]–[63]. The aim is to enable Enhanced Mobile Broadband (eMBB) services to be available everywhere and anytime with excellent service quality. But, 6G and some satellite systems operate based on mm-wave bands. That will raise mobility issues [64]–[66]. Therefore, studying self-optimization techniques with such networks will be one of the significant research targets that need to be conducted in future.
- **Optimization with Mobile Communications Growth**: The number of mobile communications will massively increase in the future leading to ultra-dense networks. That, in turn, will lead to a significant increase in the need for load balancing operation. That means further self-optimization operation will be conducted to balancing load between cells. Optimization operations and signaling overhead may increase too, thus, studying handover-self optimization with such a system is a significant part that needs to be addressed.
- **Investigating Further Algorithms**: There are several algorithms that have been proposed in the literature to automatically optimize HCPs with different scenarios. But there is no comprehensive study that can investigate all algorithms utilizing the same simulation environments to find out which models perform better. Thus, further algorithms from the literature need to be investigated to broaden the investigation further and find out the most suitable algorithms available in the literature.
- **Enabling Machine Learning (ML):**Enabling ML to be part of the solution 5G networks is one of the targeted tasks that need to be achieved. There are some works are conducted now by the International Telecommunication Union (ITU) that focusing on AI/ML in 5G Challenge [67]. Also, standardization organizations, universities and developers are working on that to enabling ML and AI technologies to be incorporated in addressing the challenges of 5G networks. Focusing on handover self-optimization based on ML will be one of the interesting research areas.

VIII. CONCLUSION

In this study, a new algorithm was proposed to dynamically estimate the HCP settings based on the WPF. The WPF estimated the optimization values according to the UE's SINR level, cell loads, and UE's speed. Furthermore, the proposed algorithm provides freedom to the serving network by independently adjusting the HCP values for each UE. Thus, each UE acquires different HCPs settings than other UEs. These HCP optimization settings were validated over various mobile speed scenarios in the 5G network. The performances were assessed in terms of RSRP, HOP, HPPP, and RLF. The simulation results have shown that the proposed algorithm achieved noticeable enhancements compared to the Dis, FLC, and HPI algorithms. As a result, the proposed algorithm can

TABLE 3. List of abbreviations in alphabetical order.

Item	Description
3GPP	3rd Generation Partnership Project
4G	Fourth Generation
5G	Fifth Generation
6G	Sixth Generation
AWF	Automatic Weight Function
BS	Base Statio
CA	Carrier Aggregation
CCI	Co-Channel Interference
CDF	Cumulative Distribution Function
DCP	Drop Call Probability
DMM	Directional Mobility Model
eMBB	enable Enhanced Mobile Broadband
EMSE	Enhanced Mobility State Estimation
eNB	evolved NodeB
FLC	Fuzzy Logic Controller
HCPs	Handover Control Parameters
HFP	Handover Failure Probability
HOM	Handover Margin
HOP	Handover Probability
HOR	Handover Ratio
HPI	Handover Performance Indicator
HPPP	Handover Ping-Pong Probability
HPSO	Handover Parameter Self-Optimization
IDHPO-AWF	Dynamic Handover Parameter Optimization algorithm based on an Automatic Weight Function
IMT-2020	International Mobile Telecommunications 2020
ITU	International Telecommunication Union
KPIs	Key Performance Indicators
LBO	Load Balancing Self-Optimization
LTE	Long Term Evolution
MCS	Modulation and Coding Scheme
ML	Machine Learning
MR	Measurement Report
MRO	Mobility Robustness Optimization
NAS	Non-access stratum
OPEX	Operating Expenditure
Rel.	Release
RLF	Radio Link Failure
RRC	Radio Resource Control
RSRP	Reference Signal Received Power
SINR	Signal-to-Interference-plus-Noise-Ratio
SON	Self-Optimization Network
TTT	Time-to-Trigger
UE's	User Equipment
WF	Weight Function
WPHPO	Handover Parameter Optimization

be recommended for implementation in 5G networks. Further investigations for proposed algorithm are needed to validate its performance. Moreover, additional investigations of the benchmark algorithms are also required to clearly show the high performance of our proposed algorithm. This will be more apparent when enabling other algorithms (found in the literature and with accurate central optimization operations) in the developed simulation model. Further investigations with other algorithms from the literature, new scenarios, and additional improvements to the simulation model will be conducted in our future study.

APPENDIX

See Table 3.

REFERENCES

[1] I. Shayea, M. Ergen, M. H. Azmi, S. A. Colak, R. Nordin, and Y. I. Daradkeh, "Key challenges, drivers and solutions for mobility management in 5G networks: A survey," *IEEE Access*, vol. 8, pp. 172534–172552, 2020.

[2] *Self-Configuring and Self-Optimizing Network (SON) Use Cases and Solutions (Release 9)*, document TR 36.902 V9.3.1, Paris, France, 3GPP, 2011.

[3] *Further Advancements for E-UTRA (LTE-Advanced) (Release 15)*, document TR 36.912 V15.0.0, 3GPP, Valbonne, France, 2018.

[4] *Self-Organizing Networks (SON) Policy Network Resource Model (NRM) Integration Reference Point (IRP); Requirements (Release 15)*, document TS 28.627 V15.0.0, 3GPP, Valbonne, France, 2018.

[5] *Self-Organizing Networks (SON) Policy, Network Resource Model (NRM), Integration Reference Point (IRP); Information Service (IS) (Release 15)*, document TS 28.628 V15.0.0, 3GPP, Valbonne, France, 2018.

[6] 3GPP, unpublished.

[7] *Telecommunication Management; Self-Organizing Networks (SON) Policy Network Resource Model (NRM) Integration Reference Point (IRP); Requirements (Release 11)*, document TS 32.521 V11.1.0, 3GPP, Valbonne, France, 2012.

[8] *Telecommunication management; Self-Organizing Networks (SON) Policy Network Resource Model (NRM) Integration Reference Point (IRP); Information Service (IS) (Release 11)*, document TS 32.522 V11.7.0, 3GPP, Valbonne, France, 2013.

[9] N. Amirrudin, S. H. S. Ariffin, N. N. N. A. Malik, and N. E. Ghazali, "Analysis of handover performance in LTE femtocells network," *Wireless Pers. Commun.*, vol. 97, no. 2, pp. 1929–1946, Nov. 2017.

[10] M. Ruggieri, D. Giancristofaro, F. Graziosi, and F. Santucci, "Design of handover procedures for mobile cellular systems through performance charts," *Wireless Pers. Commun.*, vol. 5, pp. 51–73, Jul. 1997.

[11] D. Castro-Hernandez and R. Paranjape, "Optimization of handover parameters for LTE/LTE—A in-building systems," *IEEE Trans. Veh. Technol.*, vol. 67, no. 6, pp. 5260–5273, Jun. 2018.

[12] B. Sas, K. Spaey, and C. Blondia, "A SON function for steering users in multi-layer LTE networks based on their mobility behaviour," presented at the IEEE 81st Veh. Techn. Conf. (VTC Spring), 2015.

[13] R. P. Ray and L. Tang, "Hysteresis margin and load balancing for handover in heterogeneous network," *Int. J. Future Comput. Commun.*, vol. 4, p. 231, Aug. 2015.

[14] S. Nie, D. Wu, M. Zhao, X. Gu, L. Zhang, and L. Lu, "An enhanced mobility state estimation based handover optimization algorithm in LTE—A self-organizing network," *Procedia Comput. Sci.*, vol. 52, pp. 270–277, 2015.

[15] P. Muñoz, R. Barco, and I. de la Bandera, "On the potential of handover parameter optimization for self-organizing networks," *IEEE Trans. Veh. Technol.*, vol. 62, no. 5, pp. 1895–1905, Jun. 2013.

[16] W. Zheng, H. Zhang, X. Chu, and X. Wen, "Mobility robustness optimization in self-organizing LTE femtocell networks," *EURASIP J. Wireless Commun. Netw.*, vol. 2013, no. 1, pp. 1–10, Dec. 2013.

[17] I. M. Bălan, B. Sas, T. Jansen, I. Moerman, and K. Spaey, "An enhanced weighted performance-based handover parameter optimization algorithm for LTE networks.," *EURASIP J. Wireless Commun. Networking.*, vol. 2011, pp. 1–11, Dec. 2011.

[18] K. Kitagawa, T. Komine, T. Yamamoto, and S. Konishi, "A handover optimization algorithm with mobility robustness for LTE systems," in *Proc. IEEE 22nd Int. Symp. Pers., Indoor Mobile Radio Commun.*, Sep. 2011, pp. 1647–1651.

[19] L. Ewe and H. Bakker, "Base station distributed handover optimization in LTE self-organizing networks," in *Proc. IEEE 22nd Int. Symp. Pers., Indoor Mobile Radio Commun.*, Sep. 2011, pp. 243–247.

[20] A. Awada, B. Wegmann, D. Rose, I. Viering, and A. Klein, "Towards self-organizing mobility robustness optimization in inter-RAT scenario," in *Proc. IEEE 73rd Veh. Technol. Conf. (VTC Spring)*, May 2011, pp. 1–5.

[21] G. H. P. Legg and J. Johansson, "A simulation study of LTE intra-frequency handover performance," presented at the IEEE 72nd Veh. Technol. Conf. Fall (VTC Fall), 2010.

[22] L. Yejee, S. Bongjhin, L. Jaechan, and D. Hong, "Effects of time-to-trigger parameter on handover performance in SON-based LTE systems," presented at the 16th Asia–Pacific Conf. Commun. (APCC), 2010.

[23] Q. Song, Z. Wen, X. Wang, L. Guo, and R. Yu, "Time-adaptive vertical handoff triggering methods for heterogeneous systems," presented at the Int. Workshop Adv. Parallel Process. Technol., 2009.

[24] A. Schröder, H. Lundqvist, and G. Nunzi, "Distributed self-optimization of handover for the long term evolution," presented at the Int. Workshop Self-Organizing Syst., 2008.

[25] J. Park and Y. Lim, "A handover prediction model and its application to link layer triggers for fast handover," *Wireless Pers. Commun.*, vol. 52, no. 3, pp. 501–516, Feb. 2010.

[26] M. A. Ben-Mubarak, B. Mohd. Ali, N. K. Noordin, A. Ismail, and C. K. Ng, "Fuzzy logic based self-adaptive handover algorithm for mobile WiMAX," *Wireless Pers. Commun.*, vol. 71, no. 2, pp. 1421–1442, Jul. 2013.

[27] A. Alhammadi, M. Roslee, M. Y. Alias, I. Shayea, S. Alraih, and K. S. Mohamed, "Auto tuning self-optimization algorithm for mobility management in LTE—A and 5G HetNets," *IEEE Access*, vol. 8, pp. 294–304, 2020.

[28] K. Da Costa Silva, Z. Becvar, and C. R. L. Frances, "Adaptive hysteresis margin based on fuzzy logic for handover in mobile networks with dense small cells," *IEEE Access*, vol. 6, pp. 17178–17189, 2018.

[29] I. Shayea, M. Ismail, R. Nordin, H. Mohamad, T. A. Rahman, and N. F. Abdullah, "Novel handover optimization with a coordinated contiguous carrier aggregation deployment scenario in LTE-advanced systems," *Mobile Inf. Syst.*, vol. 2016, pp. 1–20, Dec. 2016.

[30] I. Shayea, M. Ismail, R. Nordin, M. Ergen, N. Ahmad, N. F. Abdullah, A. Alhammadi, and H. Mohamad, "New weight function for adapting handover margin level over contiguous carrier aggregation deployment scenarios in LTE-advanced system," *Wireless Pers. Commun.*, vol. 108, no. 2, pp. 1179–1199, Sep. 2019.

[31] A. Alhammadi, M. Roslee, M. Y. Alias, I. Shayea, and A. Alquhali, "Velocity-aware handover self-optimization management for next generation networks," *Appl. Sci.*, vol. 10, no. 4, p. 1354, Feb. 2020.

[32] A. Alhammadi, M. Roslee, M. Y. Alias, I. Shayea, and S. Alraih, "Dynamic handover control parameters for LTE-A/5G mobile communications," in *Proc. Adv. Wireless Opt. Commun. (RTUWO)*, 2018, pp. 39–44.

[33] *Self-Organizing Networks (SON) Policy Network Resource Model (NRM) Integration Reference Point (IRP); Information Service (IS) (Release 15)*, document TS 28.628 V15, 3GPP, Valbonne, Franch, 2019.

[34] M. Li, H. Wang, and H. Wang, "Resilience assessment and optimization for urban rail transit networks: A case study of Beijing subway network," *IEEE Access*, vol. 7, pp. 71221–71234, 2019.

[35] J. Zhu, M. Zhao, and S. Zhou, "An optimization design of ultra dense networks balancing mobility and densification," *IEEE Access*, vol. 6, pp. 32339–32348, 2018.

[36] X. Xu, X. Tang, Z. Sun, X. Tao, and P. Zhang, "Delay-oriented cross-tier handover optimization in ultra-dense heterogeneous networks," *IEEE Access*, vol. 7, pp. 21769–21776, 2019.

[37] *Evolved Universal Terrestrial Radio Access Network; Self-Configuring and Self-Optimizing Network (SON) Use Cases and Solutions (Release 9)*, document TR 36.902 V9.3.1, 3GPP, Valbonne, France, Mar. 2011. [Online]. Available: http://www.3gpp.org/

[38] I. Shayea, M. Ismail, R. Nordin, and H. Mohamad, "Handover performance over a coordinated contiguous carrier aggregation deployment scenario in the LTE-advanced system," *Int. J. Veh. Technol.*, vol. 2014, 2014.

[39] I. Shayea, M. Ismail, R. Nordin, and H. Mohamad, "Adaptive handover decision algorithm based on multi-influence factors through carrier aggregation implementation in LTE-advanced system," *J. Comput. Netw. Commun.*, vol. 2014, pp. 1–8, Jan. 2014.

[40] *Carrier Aggregation; Base Station (BS) Radio Transmission and Reception (Release 10)*, document TR 36.808 V10.1.0, Valbonne, France, 2013. [Online]. Available: http://www.3gpp.org/dynareport/36808.htm

[41] *LTE Advanced Intra-band Non-contiguous Carrier Aggregation in Band 4 Work Item Technical Report (Release 12)*, document TR 36.833 V0.2.0, 3GPP, Valbonne, France, 2013. [Online]. Available: http://www.3gpp.org/dynareport/36833.htm

[42] M. Boujelben, S. B. Rejeb, and S. Tabbane, "Son handover algorithm for green LTE-A/5G HetNets," *Wireless Pers. Commun.*, vol. 95, pp. 4561–4577, Aug. 2017.

[43] H.-S. Park, Y.-S. Choi, B.-C. Kim, and J.-Y. Lee, "LTE mobility enhancements for evolution into 5G," *ETRI J.*, vol. 37, pp. 1065–1076, Dec. 2015.

[44] C.-H. Lee, S.-H. Lee, K.-C. Go, S.-M. Oh, J. S. Shin, and J.-H. Kim, "Mobile small cells for further enhanced 5G heterogeneous networks," *ETRI J.*, vol. 37, no. 5, pp. 856–866, Oct. 2015.

[45] Y. Ouyang, Z. Li, L. Su, W. Lu, and Z. Lin, "Application behaviors driven self-organizing network (SON) for 4G LTE networks," *IEEE Trans. Netw. Sci. Eng.*, vol. 7, no. 1, pp. 3–14, Jan. 2020.

[46] 3GPP. (2018). *Release 16*. Accessed: Oct. 10, 2020. [Online]. Available: http://www.3gpp.org/release-16

[47] S. Parkvall. (Jun. 2015). *Release 14—The Start of 5G Standardization*. [Online]. Available: https://www.ericsson.com/en/blog/2015/6/release-14–the-start-of-5g-standardization

[48] 3GPP. (Jun. 10, 2020). *Releases*. [Online]. Available: https://www.3gpp.org/3gpp-calendar/44-specifications/releases

[49] M. Ergen, P. Uberoy, T. Mak, and R. Jalil, "Method and apparatus for load balancing in a wireless communication network," U.S. Patent 8 849 275, Sep. 14, 2014.

[50] *Radio Frequency (RF) System Scenarios (Release 15)*, document TR 25.942 V15.0.0, 3GPP, Valbonne, France, 2018.

[51] *Radio Resource Control (RRC); Protocol Specification (Release 15)*, document TS 36.331 V15.3.0, 3GPP, 2018.

[52] *Radio Resource Control (RRC); Protocol Specification (Release 15)*, document TS 36.300 V15.3.0, 3GPP, Valbonne, France, 2018.

[53] 3GPP. (2014). *V0.1.4. Overview of 3GPP Release 12*. [Online]. Available: http://www.3gpp.org/specifications/releases/68-release-12

[54] *UMTS 900 MHz Work Item Technical Report (Release 8)*, document TR 25.816 V8.0.0, 3GPP, Valbonne, Franch, 2009. [Online]. Available: http://www.3gpp.org/DynaReport/25816.htm

[55] *Physical Layer Aspects for Evolved Universal Terrestrial Radio Access (UTRA) (Release 7)*, document TR 25.814 V7.1.0, Valbonne, Franch, 2006. [Online]. Available: http://www.3gpp.org/DynaReport/25814.htm

[56] *Study for Enhanced Uplink for UTRA FDD (Release 6)*, document TR 25.896 V6.0.0, 3GPP, Valbonne, Franch, 2014. [Online]. Available: http://www.3gpp.org/DynaReport/25896.htm

[57] M. Gudmundson, "Correlation model for shadow fading in mobile radio systems.," *Electron. Letters.*, vol. 27, pp. 2145–2146, Nov. 1991.

[58] A. Goldsmith, *Wireless Communications*. Cambridge, U.K.: Cambridge Univ. Press, 2005.

[59] B. Sklar, "Rayleigh fading channels in mobile digital communication systems. I. Characterization," *IEEE Commun. Mag.*, vol. 35, pp. 90–100, 1997.

[60] *Physical Channels and Modulation (Release 12)*, document TS 36.211 V16.1.0, 3GPP, Valbonne, France, 2020. [Online]. Available: http://www.3gpp.org

[61] M. Giordani and M. Zorzi, "Satellite communication at millimeter waves: A key enabler of the 6G era," in *Proc. Int. Conf. Comput., Netw. Commun. (ICNC)*, Feb. 2020, pp. 383–388.

[62] B. Zong, C. Fan, X. Wang, X. Duan, B. Wang, and J. Wang, "6G technologies: Key drivers, core requirements, system architectures, and enabling technologies," *IEEE Veh. Technol. Mag.*, vol. 14, no. 3, pp. 18–27, Sep. 2019.

[63] M. Abo-Zeed, J. B. Din, I. Shayea, and M. Ergen, "Survey on land mobile satellite system: Challenges and future research trends," *IEEE Access*, vol. 7, pp. 137291–137304, 2019.

[64] A. M. Al-Samman, T. A. Rahman, M. H. Azmi, and I. Shayea, "Path loss model and channel capacity for UWB–MIMO channel in outdoor environment," *Wireless Pers. Commun.*, vol. 107, pp. 1–11, Jul. 2019.

[65] I. Shayea, T. Abd. Rahman, M. Hadri Azmi, and A. Arsad, "Rain attenuation of millimetre wave above 10 GHz for terrestrial links in tropical regions," *Trans. Emerg. Telecommun. Technol.*, vol. 29, no. 8, p. e3450, Aug. 2018.

[66] I. Shayea, "Rain attenuation and worst month statistics verification and modeling for 5G radio link system at 26 GHz in Malaysia," *Trans. Emerg. Telecommun. Technol.*, vol. 30, p. e3697, Dec. 2019.

[67] ITU. (2020). *ITU AI/ML in 5G Challenge*. Accessed: Jul. 20, 2020. [Online]. Available: https://www.itu.int/en/ITU-T/AI/challenge/2020/Pages/default.aspx

IBRAHEEM SHAYEA received the bachelor's degree in electronics and communication engineering from the Faculty of Engineering, University of Diyala, Iraq, in July 2004, and the master's degree in communication and computer engineering and the Ph.D. degree in the field of electrical and electronic engineering, specifically in wireless communication systems, from the Department of Electrical, Electronic Engineering, Faculty of Engineering and Built Environment, Universiti Kebangsaan Malaysia (UKM), Malaysia, in December 2015 and in July 2010, respectively. From January 2011 to December 2015 (during his Ph.D. study), he worked as a Research Assistant and a Demonstrator with the Department of Electrical, Electronic Engineering, Faculty of Engineering and Built Environment, Universiti Kebangsaan Malaysia (UKM), Malaysia. From January 2016 to June 2018, he worked as a Postdoctoral Fellow at the Wireless Communication Center (WCC), University of Technology Malaysia (UTM), Malaysia. From September 2018 to August 2019, he worked as a Researcher Fellow with Istanbul Technical University (ITU). He is currently an Associate Researcher with the Department of Electronics and Communications Engineering, Faculty of Electrical and Electronics Engineering, Istanbul Technical University (ITU), Istanbul, Turkey, where he is also teaching courses for master's and bachelor's students. The key focuses of his research areas include mobility management in future heterogeneous (4G, 5G, and 6G) networks, mobile edge computing, machine, and deep learning, the Internet of Things (IoT), propagation of millimeter-wave, mobile broadband technology, and future data traffic growth and spectrum gap analysis. He has published several scientific research journals, conference papers, and whitepapers.

MUSTAFA ERGEN received the B.S. degree in electrical engineering, as a Valedictorian, from ODTU, the M.S. and Ph.D. degrees in electrical engineering from UC Berkeley, and the M.A. degree in international studies and MOT Program from the HAAS Business School. He is currently a Professor with Istanbul Technical University. Previously, he was with Turk Telekom, as the Chief Technology Advisor. Earlier, he co-founded Silicon Valley startup WiChorus Inc., focusing on 4G technologies and company is acquired by Tellabs [now Coriant]. Prior to this, he was a National Semiconductor Fellow [now TI] with the University of California at Berkeley, where he co-founded the Distributed Sensing Laboratory, focusing on statistical sensor intelligence and vehicular communication. He is also the Founder of venture funded Ambeent Inc., focusing on 5G WiFi and AI. He has more than 50 patent applications, many publications, and authored three books "*Mobile Broadband*" (Springer) and "*Multi-Carrier Digital Communications*" (Springer) that are about wireless communications, and the last one is about entrepreneurship, titled "*Entrepreneurial Capital: Silicon Valley History and Startup Economy*" (Alfa), a Turkish publishing company.

AZIZUL AZIZAN received the B.Eng. degree (Hons.) in electronics engineering (majoring in telecommunications) from Multimedia University, Malaysia, in 2002, and the Ph.D. degree in the area of 3.5G physical layer adaptation for satellite systems from the University of Surrey, U.K., in 2009. Later, he joined the Malaysian Communication and Multimedia Commission for more than six years overseeing spectrum and numbering policies and telecommunications resource management administration. He is currently with the Advance Informatics Department, Razak Faculty of Technology and Informatics, UniversitiTeknologi Malaysia, where his research areas include Wireless communications, edge computing, cyberphysical systems, business intelligence, and STEM education.

MAHAMOD ISMAIL (Senior Member, IEEE) received the B.Sc. degree in electrical and electronics from the University of Strathclyde, U.K., in 1985, the M.Sc. degree in communication engineering and digital electronics from UMIST, Manchester, U.K., in 1987, and the Ph.D. from the University of Bradford, U.K. He is currently a Professor with the Department of Electrical, Electronics and System Engineering, and attach to the Center for Information Technology, as the Deputy Director of Research and Education at Universiti Kebangsaan Malaysia. From 1997 to 1998, he was with the team engineer building the first Malaysian microsatellite Tiungsat in Surrey Satellite Technology Ltd., U.K. He became a Guest Professor with the University of Duisburg-Essen (formerly known as Gerhard Mercator Universität Duisburg), Germany, in Summer 2002. His research interests include mobile communication and wireless networking. He published more than 800 technical articles in journal and proceeding at local and international level. He is the past Chapter Chair of IEEE Communication Society, Malaysia, and the Educational Activities Chairman of IEEE Malaysia Section, and is currently a Committee Member of the Joint chapter Communication and Vehicular Technology Society, IEEE Malaysia. He is also actively involved in conference and became the Technical Program Chairman of technical committee and paper reviewer.

YOUSEF IBRAHIM DARADKEH received the Ph.D. degree and the Doctor of Engineering Sciences in computer engineering and information technology (computer systems engineering and computer software engineering). He is currently an Associate Professor with the Department of Computer Engineering and Networks, College of Engineering, Prince Sattam Bin Abdulaziz University, Saudi Arabia. He is also a Senior Scientific Researcher and the Assistant Dean of Administrative Affairs. He is a dynamic academician having more than 15 years of experience, specializing in teaching and scientific research development and administration experience. He has taught wide spectrum of computer science, computer engineering and networks, computer software engineering courses for undergraduate and graduate students. He has been working as a Postdoctoral Research Fellow with the Department of Electrical and Computer Engineering, University of Calgary, Canada. He is a well-known and respected scientist internationally. He also holds the P.Eng. certification. He has an excellent experience in designing courses that bridge the gap between academia and industry as well as follow the accreditation requirements. He has published over 90 high quality refereed research papers in the international journals and conferences. He has also published two books, one chapter, and an edited book in the most prestigious publications. He is a member of The International Academy of Science and Engineering for Development (IASED). The international recognition of his scientific achievements is demonstrated by numerous invitations to participate in the program committees of international conferences and foreign journals, as well as lecturing at renowned scientific centers around the world.